ARO 23338.5-CH

(2)



# DETERMINATION OF THE MECHANISM OF DECOMPOSITION OF ENERGETIC MOLECULES

Final Technical Report
Covering the Period 1 February 1986 to 31 January 1989

December 1989

By: Donald F. McMillen, Jay B. Jeffries,
Paul H. Stewart, Jean-Michel Zellweger,
Alan B. McEwen, and David M. Golden

Prepared for:

Department of the Army
U.S. Army Laboratory Command
Army Research Office
P.O. Box 12211
Research Triangle Park, NC 27709

Attention: Dr. Richard J. Paur

Contract No. DAAL03-86-K-0030
SRI Project PYU-1745

SRI International
333 Ravenswood Avenue
Menlo Park, California 94025-3493
(415) 326-6200
TWX: 910-373-2046
Telex: 334486

SRI International®

SRI International

# DETERMINATION OF THE MECHANISM OF DECOMPOSITION OF ENERGETIC MOLECULES

Final Technical Report
Covering the Period 1 February 1986 to 31 January 1989

December 1989

By: Donald F. McMillen, Jay B. Jeffries,
Paul H. Stewart, Jean-Michel Zellweger,
Alan B. McEwen, and David M. Golden

Prepared for:

Department of the Army
U.S. Army Laboratory Command
Army Research Office
P.O. Box 12211
Research Triangle Park, NC 27709

Attention: Dr. Richard J. Paur

Contract No. DAAL03-86-K-0030
SRI Project PYU-1745

Approved by:

David M. Golden, Laboratory Director
Chemistry Laboratory

G. R. Abrahamson
Senior Vice President
Sciences Group



SRI International®

# REPORT DOCUMENTATION PAGE

| | |
|---|---|
| 1a. REPORT SECURITY CLASSIFICATION: UNCLASSIFIED | 1b. RESTRICTIVE MARKINGS |
| 2a. SECURITY CLASSIFICATION AUTHORITY: NA | 3 DISTRIBUTION / AVAILABILITY OF REPORT: UNCLASSIFIED |
| 2b. DECLASSIFICATION / DOWNGRADING SCHEDULE: NA | |
| 4. PERFORMING ORGANIZATION REPORT NUMBER(S): PYU-1745 | 5. MONITORING ORGANIZATION REPORT NUMBER(S): ARO 23338.5-CH |
| 6a. NAME OF PERFORMING ORGANIZATION: SRI International; 6b. OFFICE SYMBOL (If applicable) | 7a. NAME OF MONITORING ORGANIZATION: U.S. Army Research Office |
| 6c. ADDRESS (City, State, and ZIP Code): 333 Ravenswood Avenue, Menlo Park, CA 94025-3493 | 7b. ADDRESS (City, State, and ZIP Code): P.O. Box 12211, Research Triangle Park, NC 27709 |
| 8a. NAME OF FUNDING / SPONSORING ORGANIZATION; 8b OFFICE SYMBOL (If applicable) | 9. PROCUREMENT INSTRUMENT IDENTIFICATION NUMBER: DAAL03-86-K-0030 |
| 9c. ADDRESS (City, State, and ZIP Code) | 10. SOURCE OF FUNDING NUMBERS: PROGRAM ELEMENT NO. / PROJECT NO / TASK NO / WORK UNIT ACCESSION NO |

11. TITLE (Include Security Classification)
DETERMINATION OF THE MECHANISM OF DECOMPOSITION OF ENERGETIC MOLECULES

12. PERSONAL AUTHOR(S)
D.F.McMillen, Jay B.Jeffries, Paul H.Stewart, Jean-Michel Zellweger, A.B. McEwen, and D.M.Golden

| 13a. TYPE OF REPORT | 13b. TIME COVERED | 14. DATE OF REPORT (Year, Month, Day) | 15. PAGE COUNT |
|---|---|---|---|
| Final Technical | FROM 860201 TO 890131 | 8912 | 55 |

16. SUPPLEMENTARY NOTATION

| 17 COSATI CODES | | |
|---|---|---|
| FIELD | GROUP | SUB-GROUP |
| 07 | 04 | |
| 19 | 01 | |

18. SUBJECT TERMS (Continue on reverse if necessary and identify by block number)
Propellants, nitramines, dimethylnitramine, chemical decomposition, mechanisms, rates, initial steps, laser-pyrolysis.

19. ABSTRACT (Continue on reverse if necessary and identify by block number)

As a prototype for more complex nitramines, the gas-phase decomposition of dimethylnitramine was studies in three laser-pyrolysis systems. Results in two of these systems, unlike those reported in the literature, indicate that a nitro-nitrite rearrangement pathway is competitive with the expected (and previously invoked) $NNO_2$ bond scission. This rearrangement pathway has been obscure because it can lead to some of the same products that are yielded by the bond scission route. The principal evidence for nitro-nitrite rearrangement includes (1) Arrhenius parameters for decomposition (log k/s = 13.5 $\pm$ 0.6 - 37.4 $\pm$ 2.5 /2.3 RT) that are two orders of magnitude too low to be consistent with simple $N-NO_2$ bond scission as the sole rate-determining step, (2) molecular-beam, mass-spectrometrically sampled laser pyrolysis studies that show direct detection of NO and the nitroxyl radical $(CH_3)_2NO\cdot$ on a time scale too short to allow for the production of these substances in secondary bimolecular reactions, and (3) ab initio calculations (in concurrent AFOSR-funded work) that find a rearrangement pathway at slightly lower energy than

| | |
|---|---|
| 20. DISTRIBUTION / AVAILABILITY OF ABSTRACT: ☒ UNCLASSIFIED/UNLIMITED ☐ SAME AS RPT. ☐ DTIC USERS | 21. ABSTRACT SECURITY CLASSIFICATION: UNCLASSIFIED |
| 22a. NAME OF RESPONSIBLE INDIVIDUAL: Richard J. Paur | 22b. TELEPHONE (Include Area Code): (919)549-0651; 22c. OFFICE SYMBOL |

DD FORM 1473, 84 MAR — 83 APR edition may be used until exhausted. All other editions are obsolete.

SECURITY CLASSIFICATION OF THIS PAGE
UNCLASSIFIED

19. Abstract (concluded)

that of simple bond scission. These results suggest that such rearrangement pathways may be a common feature of nitramine decomposition, as other studies have recently shown them to be for C-$NO_2$ compounds.

Because of these experimental and theoretical results for dimethylnitramine, we embarked on an extra effort to use laser-induced fluorescence to determine, on a microsecond time scale, the branching between initial decomposition steps producing NO and $NO_2$. Due to omplications from CN chemiluminescence, this effort was not completed by the end of the project, but did succeed in delineating the extent of the complications and laying the groundwork for successful LIF measurements of the NO-$NO_2$ branching ratio. Since all the other approaches in this project point to the conclusion that a nitro-nitrite rearrangement pathway for dimethylnitramine is competitive with N-$NO_2$ bond scission at temperatures of about 900 K, we recommend that this rearrangement be considered a potential contributor to the decomposition of other nitramines.

In repeated syntheses of dimethylnitramine, we also developed a new method of synthesis via the nitrodephosphorylation of phosphoramides, which offers substantial convenience and safety features for certain nitramines.


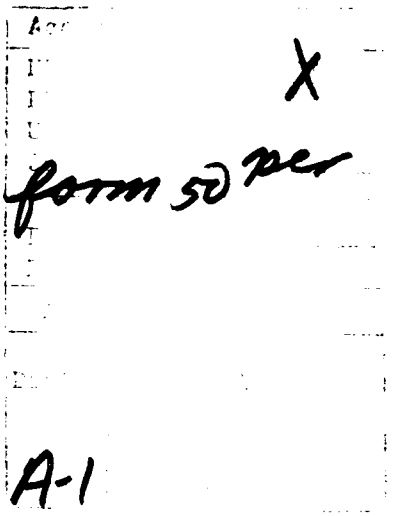

# CONTENTS


INTRODUCTION ..... 1

LASER PYROLYSIS OF DIMETHYLNITRAMINE AND DIMETHYLNITROSAMINE ..... 3

GC-MS-Monitored Laser-Pyrolysis ..... 6
Molecular-Beam, Mass Spectrometrically-Monitored Laser-Pyrolysis ..... 7
Laser-Induced Fluorescence Measurements of NO and $NO_2$ ..... 7

CONCLUSIONS ..... 9

REFERENCES ..... 10

APPENDICES

A THERMAL DECOMPOSITION OF DIMETHYLNITRAMINE AND DIMETHYLNITROSAMINE BY PULSED LASER PYROLYSIS

B MOLECULAR-BEAM SAMPLED LASER PYROLYSIS OF DIMETHYLNITRAMINE

C SYNTHESIS OF N,N-DIMETHYLNITRAMINE BY NITRODEPHOSPHORYLATION OF HEXAMETHYLPHOSPHORAMIDE.

D LASER-INDUCED FLUORESCENCE DETECTION OF $NO_2$ AND NO FROM THE THERMAL DECOMPOSITION OF DIMETHYLNITRAMINE

# INTRODUCTION

The principal objective of this project was to identify and measure the thermal rate parameters for the initial and/or rate-limiting steps in the gas-phase decomposition of nitramines. In support of this goal, which also received funding from the Air Force Office of Scientific Research, we applied four approaches. Experimentally, we used three laser pyrolysis systems to study the initial and secondary reactions in the decomposition of dimethylnitramine, and during the work we developed a new synthesis method for nitramines. The theoretical effort (funded solely by AFOSR) involved the use of *ab initio* quantum mechanical calculations to help determine the extent to which nitro-nitrite rearrangement is a competitive pathway in the decomposition of nitramines. The results of each of these approaches are summarized in this report and those having support from ARO are presented in detail in Appendices A through D. Appendices A and B were published in the *Journal of Physical Chemistry*, and Appendix C was published in the *Journal of Organic Chemistry*. Appendix D is a draft of a manuscript that will be submitted for publication.

As an important class of energetic materials, nitramines have been the subject of numerous studies to elucidate various facets of the chemistry that determines whether a self-sustaining reaction is achieved and, in the case of propellant compositions, determines the rate of combustion. Inasmuch as attempts to modify the burn rates of nitramine propellants have met with only very modest success, and inasmuch as the high pressure-dependence of HMX combustion rate aggravates a tendency toward instability and deflagration-to-detonation phenomena, achieving a better understanding of nitramine chemistry could have substantial practical impact. However, the chemical details of nitramine decomposition, like those for other energetic materials, have been very difficult to ascertain. This difficulty is hardly surprising because, in substances that decompose by one or more rate-limiting initial endothermic steps, followed by a sequence of highly exothermic and very rapid steps, the nature of the rate-limiting steps themselves tends to be obscured. Characterizing nitramine decomposition is particularly difficult, not only because secondary bimolecular reactions of radicals with NO2 are particularly fast, but also

because the aliphatic radicals formed from the carbon-nitrogen skeleton have a wider range of possible reactions than, for example, the typical aromatic radical produced in nitroaromatic decomposition.

Dimethylnitramine (DMNA) decomposition is not exactly analogous to decomposition of the cyclic nitramines, which have several additional pathways potentially available.[1,2] However, because previous research shows that understanding even DMNA decomposition is difficult,[3-9] we chose to study competition in the reaction pathways of DMNA before tackling RDX and HMX, which have still more complex chemistry, lower vapor pressures, and higher reactivities.

The expedient commonly used in attempts to minimize the obscuring of rate-limiting steps by rapid secondary reactions is to perform the decomposition at much lower temperatures and/or much lower pressures (concentrations) than those involved during "normal" operation. Drastically different temperature and pressure conditions are likely to cause significant shifts in competing reactions and, therefore, leave undetermined the rate-limiting steps that are actually operative under practical conditions. In our research, we lowered the pressure, but not the temperature, and used very short reaction times.

# LASER PYROLYSIS OF DIMETHYLNITRAMINE AND DIMETHYLNITROSAMINE

To help determine the rate-limiting step or steps at relevant temperatures, we chose an intermediate experimental course in which the pressure, but not the temperature, is significantly lowered and the reaction time is very short. A pulsed infrared laser is used to heat the substrate by heating an absorbing but unreactive gas (e.g., $SF_6$) that then transfers its kinetic energy by collision; in this way, the substrate is brought to high temperature (700-1200K) in 1-3 μs. Reaction then occurs in the 1 to 15 μs in which the acoustic expansion wave moves radially inward toward the center of the laser-heated region. By using different methods of sampling the product mixture, we can examine different extents of secondary reactions.

We used three techniques to determine products. One involves passing the contents of the cell shown in Figure 1 through an automatically operated gas-sampling valve, which periodically injects a sample into a GC/MS system. This technique provides a time-averaged mixture of products from the entire reaction zone and a reliable average temperature/reaction time from the simultaneously determined fractional decomposition of a temperature standard.[10-12] The second technique involves a separate apparatus (Figure 2) in which the laser-heated region is located immediately adjacent to the sampling nozzle of a molecular-beam mass spectrometric detection system. In this case, the gas mixture in the laser-heated region expands toward the nozzle, and the product mixture is frozen by the molecular-beam formation. The product mixture in the periphery of the laser-heated region has the least opportunity for secondary reaction, and that in the inner portions has progressively more opportunity. The third technique involves the use of laser-induced fluorescence (LIF) to determine, on a microsecond-timescale, the yields of NO and $NO_2$.

With the first two sampling techniques, the extent of secondary reaction can be varied by varying the substrate partial pressure, the extent of the initial reaction, and the presence of radical scavengers and radical traps. The presence of scavengers and traps has been particularly important in investigating dimethylnitramine, which, its apparent simplicity notwithstanding, has a number of initial and secondary reaction pathways open

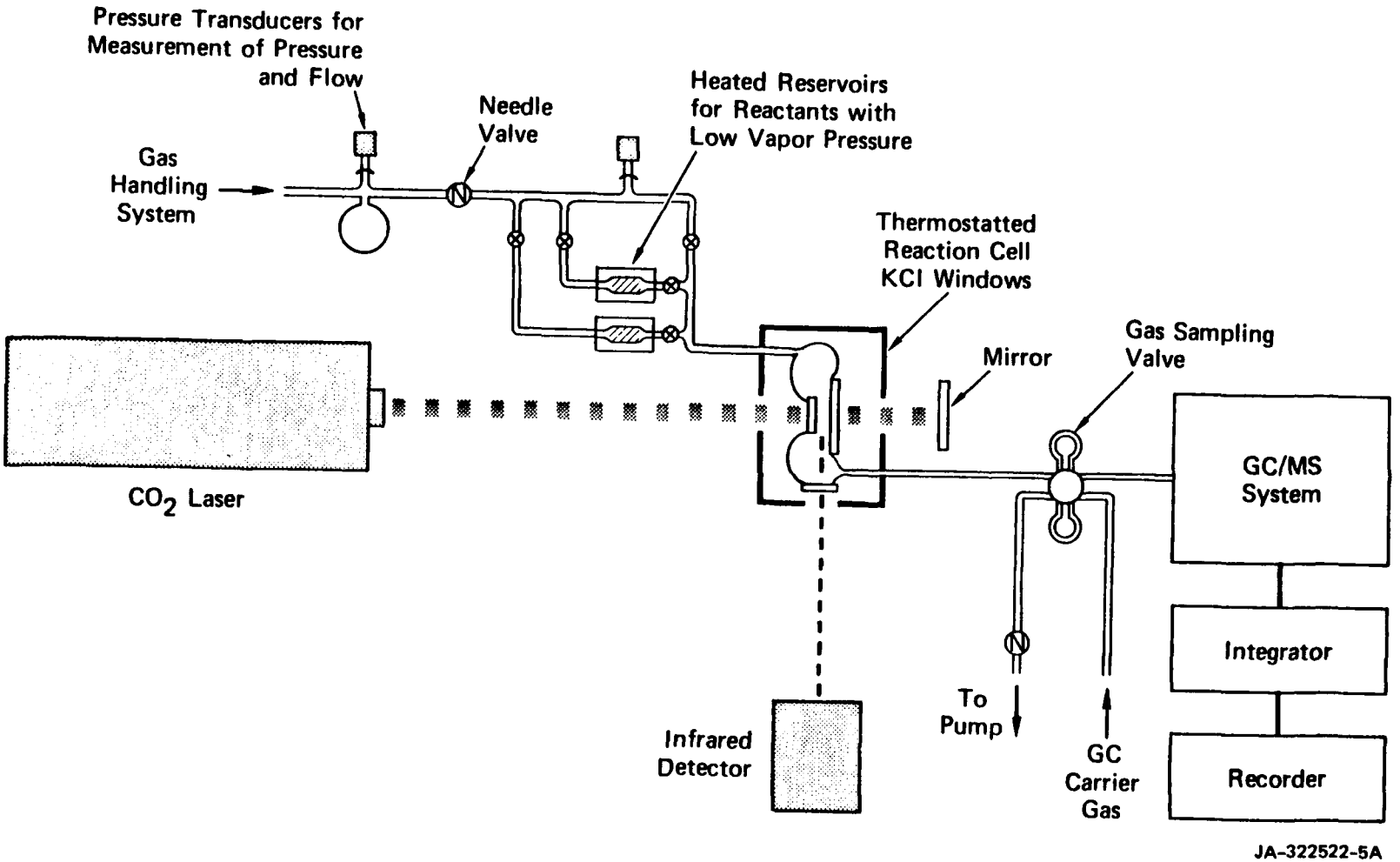


Figure 1. Schematic of gas chromatographically monitored laser-powered homogeneous pyrolysis flow system.

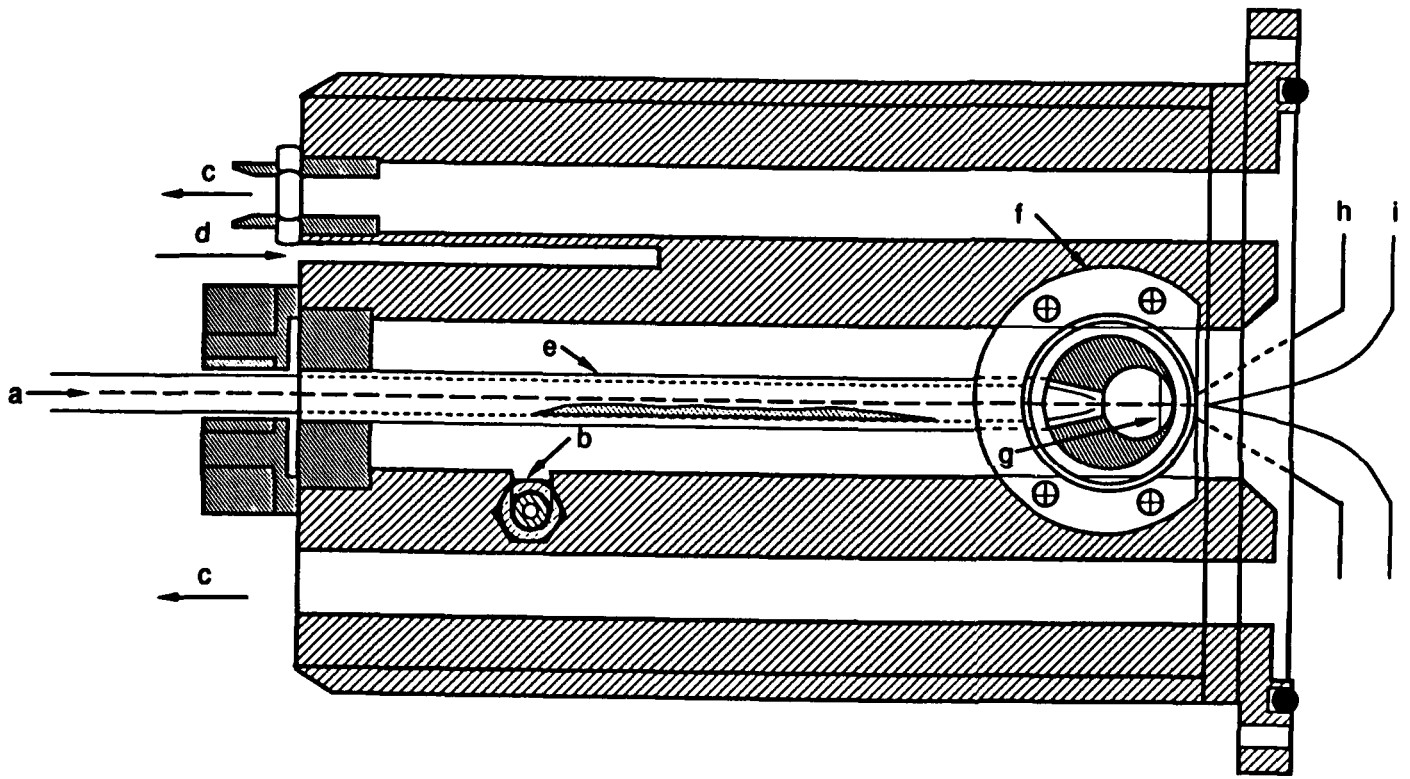


a. Carrier gas inlet
b. Dilution gas inlet
c. Flow cell pumpout
d. Well for thermometer
e. Substrate reservoir
f. Retaining ring and shroud for KCl windows
g. Location of sampling nozzle
h. Nozzle support
i. Skimmer

JA-M-8232-6

Figure 2. Schematic drawing of the machined aluminum flow cell.

to it. With the third technique, measurement of LIF signals for NO and $NO_2$ about 3 μs after the IR heating pulse entirely precludes even the fastest secondary bimolecular reactions.

## GC/MS-MONITORED LASER PYROLYSIS

DMNA was pyrolyzed over the temperature range 800 to 900K in a flow system using pulsed infrared laser heating. The major product under all conditions was dimethylnitrosamine (DMNO); smaller amounts of N-methylmethyleneimine and dimethylamine were also produced when radical scavengers and traps were not both present. Arrhenius parameters for the decomposition were log k ($s^{-1}$) = 13.5 ± 0.6 - (37.4 ± 2.5)/2.3RT. These parameters, which were produced under a wide range of conditions (different scavengers, different temperatures, and varying amounts of added NO as a trap for dimethylamino radicals), are not consistent with simple bond scission as the sole rate-limiting step.

The decomposition of principal product, DMNO, was studied under the same conditions; DMNO has no plausible decomposition pathways other than simple bond scission, and it decomposed with parameters appropriate to such a process, namely, log k ($s^{-1}$) = 15.8 ± 1.1 - (50.3 ± 3.4)/2.3RT. Moreover, the temperature dependence was evidently not distorted (as feared) by secondary reactions involving the highly reactive methyleneimine, which was the major product of DMNO decomposition, but a less important product of DMNA decomposition.

The experimental products and temperature dependence can be reproduced by a mechanistic numerical model when N-NO2 bond scission and nitro-nitrite rearrangement are competitive initial steps, and the displacement of NO2 from DMNA by NO is included as a low-temperature route to DMNO. Thus, these results lead us to conclude that DMNA decomposes not only by the expected simple bond scission reaction, but also by an intramolecular nitro-nitrite rearrangement. Such reactions have been shown to occur in C-NO2 systems,[13-14] but have not been previously reported in nitramines.

These results are described in detail in Appendix A, which was published in the *Journal of Physical Chemistry.*

## MOLECULAR-BEAM MASS-SPECTROMETRICALLY-MONITORED LASER PYROLYSIS

Because the products of an initial nitro-nitrite rearrangement can also result from a secondary bimolecular reaction in which the dimethylamino radical is oxidized by NO2, and because the evidence summarized above for the intramolecular rearrangement, while extensive, is largely indirect, we used a second laser-pyrolysis system to examine directly the products of dimethylnitramine decomposition. With this system (Figure 2), the product mixture in the laser-heated region expands directly into the nozzle of a molecular-beam sampling system and is detected by a quadrupole mass spectrometer.

The initial products include not only dimethylamino radical and NO2, but also comparable amounts of NO and various fragment ions of the nitroxyl radical $(CH_3)_2NO$. Although the bimolecular oxidation of radicals by NO2 is known to be very rapid, the NO2 partial pressure is too low and the time available before the product mixture is frozen in the expansion too short for this route to be important. In fact, when the partial pressures of initially produced NO2 and dimethylamino radicals are each increased by about a factor of ten, the consumption of NO2 in secondary bimolecular reactions becomes significant.

Calibration of the detection system using known flows of laser-heated NO and NO2 indicates that the rearrangement/N-NO2 bond scission branching ratio (at about 900K) is 0.7. Although this ratio is slightly lower than that derived from the GC-MS-monitored studies, these results generally confirm the inferences drawn from the low temperature-dependence consistently observed in those earlier studies.

This work is described in detail in Appendix B, which was published in the *Journal of Physical Chemistry*.

## LASER-INDUCED FLUORESCENCE MEASUREMENTS OF NO AND $NO_2$

The molecular-beam mass spectrometrically monitored studies resulted in the detection of NO and NO2 in the expanding laser-heated region, under conditions where the NO/NO2 ratio showed no dependence on either the starting partial pressure or the fractional decomposition of dimethylnitramine. This result indicates that the NO could not have been produced in secondary bimolecular reactions. However, the time required for the leading edge of laser-heated region to expand into the sampling orifice and for the composition to

be frozen by molecular beam formation was 5-15 μs, too long to have precluded all secondary reactions on an *a-priori* basis. Given the importance of understanding the competition between initial decomposition steps in nitramine decomposition, therefore, we decided to use laser-induced fluorescence to measure the NO and $NO_2$ yields within a few microseconds of the IR heating pulse. Although this effort was not called for in the original proposal, it was clear that the somewhat surprising (though largely self-consistent) results obtained thus far in the project warranted trying an additional approach.

In the attempt to make LIF measurements of a mixture containing both NO and $NO_2$, several potential complications were addressed. These included possible photochemical generation of NO from $NO_2$, possible photochemical decomposition of dimethylnitramine (or decomposition intermediates) to produce NO or $NO_2$, and interfering chemiluminescence resulting from decomposition of an energetic material. All but the last were successfully dealt with. The measurement of $NO_2$ in the presence of NO via 452-nm single-photon excitation did not offer significant complication. However, the measurement of NO via two-photon excitation at 452 nm has thus far been prevented by interference from intense luminescence from what is apparently a very small amount of thermally generated CN.

These results are described in Appendix D, a draft of a manuscript that will be submitted for publication when the study can be completed.

# CONCLUSIONS

The result of our three approaches to understanding dimethylnitramine decomposition is a demonstration of the existence of a new initial reaction pathway for nitramines, a unimolecular nitro-nitrite rearrangement, followed by rapid scission of the extremely weak $(Me)_2NO$-NO bond. This rearrangement pathway, which tends to be competitive with the expected N-$NO_2$ scission, is analogous to that shown recently for aliphatic and aromatic nitrocompounds, but had not been previously reported for nitramines. Recent dimethylnitramine decomposition results in the literature[7-9] had, in fact, been interpreted as evidence for exclusive N-$NO_2$ scission. The new nitro-nitrite rearrangement pathway may have relevance for the practical functioning of nitramines, since it leads directly to a more oxidized skeleton (and possibly to the various RDX nitrosamine products recently reported by Hofsommer et al. in condensed phase decomposition[15]), but may well block the concerted (or sequential) depolymerization to the nitro-imine monomer units. The importance of the latter products is that they can lead directly to $N_2O$ and formaldehyde, and thence, in a highly exothermic reaction, to $N_2$, CO, and $H_2O$.

Thus, changes in the branching ratios between nitro-nitrite rearrangement and competing initial steps (N-$NO_2$ scission and, in cyclic nitramines, depolymerization) may well help determine whether the decomposition process proceeds to a self-sustaining stage. In more general terms, the results serve to emphasize the multiplicity of pathways available to nitramines and the necessity, difficulties notwithstanding, for characterizing these pathways if the factors controlling nitramine ignition, initiation, and deflagration-to-detonation behavior are to be really understood.

# REFERENCES


1. Shaw, P.; Walker, F. E., *J. Phys. Chem.*, **1977**, *81*, 2572.

2. Schroeder, M. A., "Critical Analysis of Nitramine Decomposition Results: Some Comments on Chemical Mechanisms," in *Proc. 16th JANNAF Comb. Mtg*, CPIA, 14 September 1979, Vol. 2, p. 17.

3. Fluornoy, J. M.;,J. Chem. Phys., **1962**, *36*, 1106.

4. Korsunskii, B. L.; Dubovitskii, F.I.; Sitonina, G.V., *Doklady Akademii Nauk SSSR*, **1967**, *174(5)*, 1126.

5. Korsunskii, B. L.; Dubovitskii, F. I., *Doklady Akademii Nauk SSSR*, **1964**, *155*(2), 402.

6. McMillen, D. F.; Barker, J. R.; Lewis, K. E.; Trevor, P. L.; Golden, D. M., "Mechanisms of Nitramine Decomposition: Very Low-Pressure Pyrolysis of HMX and Dimethylnitramine," Final Report, SRI Project PYU5787, 18 June 1979 (SAN 0115/117), DOE Contract No. EY-76-C-03-0115.

7. Lloyd, S. A.; Umstead, M. E.; Lin, M. C., *J. Energetic Materials*, **1985**, *3*, 187.

8. Umstead, M. E.; Lloyd, S. A.; Lin, M. C., *Proc. 22nd JANNAF Comb. Mtg.*, CPIA, 1985, p. 512.

9. Wodtke, A. M., private communication.

10. Shaub, U. M.; Bauer, S. H., *Int. J. Chem. Kinet.*, **1975**, *7*, 509.

11. McMillen, D. F.; Lewis, K. E.; Smith, G. P.; Golden, D. M., *J. Phys. Chem.*, **1983**, *86*, 709.

12. Tsang, W., *J. Chem. Phys.*, **1964**, *40* ,1498.

13. Gonzalez, A. C.; Larson, C. W.; McMillen, D. F.; Golden, D. M., *J. Phys. Chem.*, **1985**, *89*, 4809.

14. Batt, L.; Robinson, G. N., "Thermochemistry of Nitro Compounds, Amines, and Nitroso Compounds," in *Chemistry of Functional Groups: Supplement F*, (Ed. S. Patai, J. Wiley and Sons, Ltd., Chichester, 1981) p. 1035.

15 Hoffsommer, J. C.; Glover, D. J., *Comb. Flame*, **1985**, *59*, 303.

# Appendix A

## THERMAL DECOMPOSITION OF DIMETHYLNITRAMINE DIMETHYLNITROSAMINE BY PULSED LASER PYROLYSIS

# Thermal Decomposition of Dimethylnitramine and Dimethylnitrosamine by Pulsed Laser Pyrolysis

**S. Esther Nigenda, Donald F. McMillen, and David M. Golden***

*Department of Chemical Kinetics, SRI International, Menlo Park, California 94025*
*(Received: November 30, 1987)*

Pyrolysis of dimethylnitramine (DMNA) and dimethylnitrosamine (DMNO) was carried out in a flow system over the temperature range 800–900 K using pulsed infrared laser heating, via $SF_6$ in a 250-Torr bath of $CO_2$ and radical scavenger. Arrhenius parameters for DMNO and DMNA composition were $\log k\ (s^{-1}) = (15.8 \pm 1.1) - (50.0 \pm 3.4)/2.3RT$ and $(13.5 \pm 0.6) - (37.4 \pm 2.5)/2.3RT$, respectively. The former set of parameters is consistent with simple bond scission as the rate-limiting step; the latter set, which was produced with different scavengers, temperature standards, and varying amounts of added NO as a radical trap, is not consistent with simple bond scission. The experimental results can be reproduced via a mechanistic numerical model in which N–$NO_2$ bond scission and nitro–nitrite rearrangement are competitive initial steps and the displacement of $NO_2$ from DMNA by NO is included as a low-temperature route to DMNO.

## Introduction

Some years ago Fluornoy[1] reported that the decomposition of *N,N*-dimethylnitramine in static bulb experiments over the temperature range 165–200 K resulted in formation of *N,N*-dimethylnitrosamine in roughly 80% yield. He explained this product via recombination of NO and dimethylamino radicals. This reaction is in itself completely reasonable. However, Fluornoy found it necessary to invoke reactions that would produce NO in high yield, but these are somewhat vague and questionable, as discussed by Lin.[2] Several years ago, we[3] used the very low pressure pyrolysis technique (VLPP) to examine dimethylnitramine decomposition at pressures in the milliTorr range. More recently, Lin and co-workers have studied the decomposition of dimethylnitramine in both low-temperature (466–524 K) static bulb experiments[2] and in single-pulse shock tube work at much higher temperatures (800–1200 K).[4] Lee and co-workers[5] have also recently studied the infrared multiphoton decomposition of dimethylnitramide under collisionless conditions. The results of these and other workers are summarized in Table I. In all but the two cases where the molecules are the most isolated (the multiphoton and the VLPP studies), the major product is dimethylnitrosamine. Thus, reaction leads to a product having the N–N bond intact, in spite of the fact that the initial reactions are presumed to have involved N–N bond scission of one sort or another. Re-forming the N–N bond (e.g., through radical recombination with NO) is not in itself difficult, but for it and other secondary reactions to take place at rates such that dimethylnitrosamine is produced in almost quantitative yield is a result that one would not have predicted.

The general goal of this work is to determine the products of dimethylnitrosamine decomposition and the temperature dependence of the various rate-controlling processes, in order to help achieve the overall goal of understanding what controls the decomposition of cyclic nitramines and other energetic materials. Under almost all circumstances (all but low concentrations and/or very short time scales), the nature of these materials dictates that this means considering not only the initial steps but also a varying range of secondary reactions. This paper presents our results for the thermal decomposition of dimethylnitramine and dimethylnitrosamine using GC–MS monitored laser-powered homogeneous pyrolysis (LPHP). In this technique, the net decomposition in a flow system averaged over many laser pulses and over the entire volume of the cell is measured. A mechanistic numerical model accounting for the observed Arrhenius parameters, the products, and their relative yields is also presented. Complementary results obtained with a real-time molecular beam mass spectrometrically monitored version of LPHP are the subject of a paper to be submitted.

**TABLE I: Literature Parameters for Dimethylnitramine Decomposition**

| log ($A$/s$^{-1}$) | $E$, kcal/mol | technique | $T$ range, K | $P$, Torr | ref/year |
|---|---|---|---|---|---|
| *a* | *a* | mol beam MPD | *a* | *a* | 5/1986 |
| 15.9 | 44.1 | bulb/SPST | 466–1000 | 474, 3–6 | 4/1985 |
| 16.5 ± 0.5 | 45.4 | bulb | 466–524 | 475 | 2/1985 |
| 12.4 | 37.0 | VLPP | 560–850 | $\sim 10^{-3}$ | 3/1979 |
| 13.7 | 38.9 | bulb | 450–510 | ~200 | 6/1987 |
| 14.1 | 40.8 | bulb | 450–530 | 64–400 | 7/1964 |
| 20.1 | 53.0 | bulb | 440–470 | 200–750 | 1/1961 |

[a] Product mass spectra and flight times consistent with N–$NO_2$ bond scission.

## Experimental Procedure

The pulsed laser pyrolysis technique used here (GC–MS monitored) has been described in detail.[6] Briefly, a $CO_2$ laser is used to heat the substrate (at 0.1 Torr) via an absorbing but unreactive gas (e.g., $SF_6$, ~10 Torr), which then transfers its kinetic energy by collision (total pressure 100 Torr, collision frequency $10^9$/s), bringing the substrate to high temperature in 1–3 μs. For radical-forming processes, scavengers and/or traps are necessary (e.g., toluene, cyclopentane, NO, ~5–20 Torr). Reaction then occurs in the roughly 10 μs available before cooling takes place as the acoustic expansion wave moves radially inward toward the center of the cell. Figure 1 shows a schematic of the LPHP apparatus.

With the LPHP technique, surface-catalyzed reactions at high temperatures are essentially precluded, since the time scale for heating, reaction, and cooling is far shorter than the millisecond time scale of diffusion to the walls. (Adsorption of IR-absorbing reactants or products on the KCl windows could conceivably result in decomposition of an adsorbed phase. This is generally unlikely, since only extremely strongly absorbing materials would be heated to a sufficiently high temperature when present at only a few monolayers thickness on the transparent, cold windows).

(1) Fluornoy, J. M. *J. Chem. Phys.* **1962**, *36*, 1106.
(2) Lloyd, S. A.; Umstead, M. E.; Lin, M. C. *J. Energ. Mater.* **1985**, *3*, 187.
(3) McMillen, D. F.; Barker, J. R.; Lewis, K. E.; Trevor, P. L.; Golden, D. M. "Mechanisms of Nitramine Decomposition: Very Low-Pressure Pyrolysis of HMX and Dimethylnitramine", Final Report, SRI Project PYU-5787, June 18, 1979 (SAN 0115/117). DOE Contract EY-76-C-03-0115.
(4) Umstead, M. E.; Lloyd, S. A.; Lin, M. C. In *Proceedings of the 22nd JANNAF Combustion Meeting*; CPIA: 1985; p 512.
(5) Wodtke, A. M., private communication.
(6) Korsunskii, B. L.; Dubovitskii, F. I.; Sitonina, G. V. *Dokl. Akad. Nauk SSSR* **1967**, *174*(5), 1126.
(7) Korsunskii, B. L.; Dubovitskii, F. I. *Dokl. Akad. Nauk SSSR* **1964**, *155*(2), 402.
(8) McMillen, D. F.; Lewis, K. E.; Smith, G. P.; Golden, D. M. *J. Phys. Chem.* **1982**, *86*, 709.

0022-3654/89/2093-1124$01.50/0 

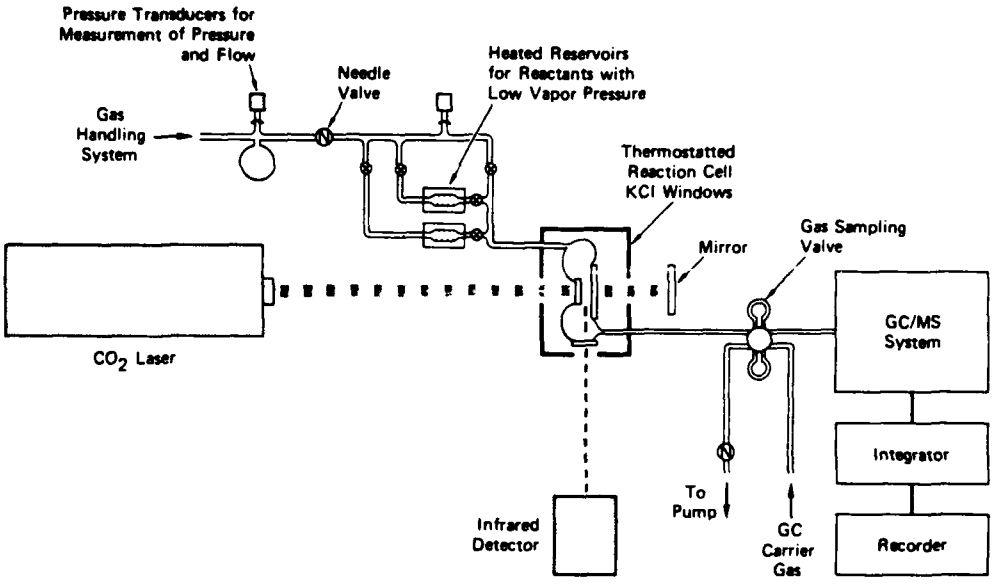


**Figure 1.** Schematic of GC–MS monitored LPHP apparatus.

The need to explicitly measure the temperature corresponding to any particular measurement of $k$ is eliminated by use of the "comparative rate" technique.[8,9] This involves concurrent determination of the fractional decomposition of a temperature standard, a second "substrate" (~0.2 Torr) whose decomposition rate temperature dependence is already well-known and therefore whose fractional decomposition defines an "effective" temperature that is a convolution of temperature over time and space within the heated portion of the cell. Given that the temperature dependence of the substrate and the temperature standard are not greatly different and that the fractional decomposition of both materials is less than about 25%, the standard and the substrate "track" the temperature variations in a similar manner. Data reduction simply involves determining the slope and intercept of a plot of log $k_{unknown}$ vs log $k_{standard}$, which correspond to the ratio of activation energies and the difference in the log $A$ values, respectively. As discussed in ref 8 and 9, uncertainties in reaction time and in cell volumes cause no error in the derived activation energies (slope of the comparative rate plot) and only small errors in derived $A$ factors.

The extent to which the comparative rate method accommodates the temperature and reaction time variations inherent in this laser pyrolysis technique has been amply demonstrated by estimates of the errors involved and by testing the technique using a series of "unknowns" whose Arrhenius parameters have already been reported in the literature.[8,9d] This has provided values in good agreement with the literature parameters for a series of molecular elimination reactions. The precision achievable indicates that the pulse-to-pulse and minute-to-minute laser variations that existed under the conditions of this experiment did not give rise to any distortion of the derived temperature dependence. Tests of this type make it clear that the comparative rate method, applied to pulsed laser pyrolysis, is very successful in accommodating the temperature variations inherent in the method and thereby providing an accurate measure of the temperature dependence of the substrate.

In this particular study, initial experimental difficulties included adsorption of substrates on the cell walls, premature decomposition of substrates, and interference by chemical impurities. These difficulties were minimized and good mass balances obtained by silanizing the entire flow system including the gas reservoirs, by carefully maintaining the lines and cell temperatures at 95 °C (at lower temperatures, adsorption occurred; at higher temperatures, preliminary decomposition occurred), and by scrupulous purification of all compounds used. In particular, traces of $NO_2$ were removed from NO by passing it through three scrubbers containing 10 M NaOH, NaOH pellets, and molecular sieves, respectively. Special care was given to the elimination of $NO_2$ from NO, since the former readily gave rise to the nitrates and nitrites of the temperature standards used, thus distorting their decomposition temperature dependence.

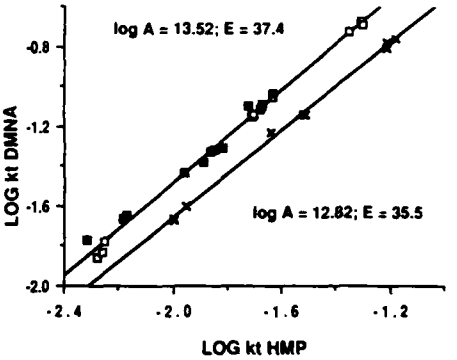


**Figure 2.** Comparative rate plot of dimethylnitramine (DMNA) vs 4-hydroxy-4-methyl-2-pentanone (HMP): (■) 50-fold excess of NO; (□) 100-fold excess of NO; (×) no additional NO; toluene as scavenger.

## Results

*Experiments.* The thermal decomposition of dimethylnitramine was studied over the temperature range 780–880 K. Figure 2 shows the decomposition rate of dimethylnitramine versus that of 4-hydroxy-4-methyl-2-pentanone (HMP) for two different experimental conditions. The rate expression[10] for HMP is log $k$ (HMP → 2-acetone) = $11.63 - 32.3/2.3RT$. In most cases an approximately 50- to 100-fold excess of radical scavenger, i.e., either toluene or cyclopentane, was used and the mass balance (decomposed material accounted for as product) for the temperature standard was 99 ± 3%.

Excess nitric oxide was used in two of the runs shown in Figure 2 in order to trap any dimethylaminyl radicals formed by the homolysis of the N–N bond in dimethylnitramine. Secondary reactions and products were thus minimized, and dimethylnitrosamine accounted for 100 ± 16% of the decomposed dimethylnitramine (for decompositions that were typically less than 10%). The least-squares line drawn through the filled and unfilled

(9) (a) Tsang, W. *J. Chem. Phys.* **1964**, *40*, 1171. (b) Tsang, W. *Ibid.* **1964**, *41*, 2487. (c) Tsang, W. *Ibid.* **1967**, *46*, 2817. (d) Shaub, W. M.; Bauer, S. H. *Int. J. Chem. Kinet.* **1975**, *7*, 509.

(10) Smith, G. G.; Yates, B. L. *J. Org. Chem.* **1965**, *30*, 2067.

**TABLE II: Laser Pyrolysis Comparative Rate Results for Dimethylnitramine**

| temp std | scavenger | x-fold excess of NO | log ($A$/s$^{-1}$) | $E_a$, kcal/mol | nitrosamine yield[a] |
|---|---|---|---|---|---|
| HMP | cyclopentane | 100 | 13.5 | 37.7 | 113 |
| HMP | toluene | 100, 50 | 13.9 | 38.0 | 99 |
| HMP | toluene | 0 | 12.8 | 35.5 | 25 |

[a] (dimethylnitrosamine)/Δ(dimethylnitramine).

squares is a composite of two runs performed under similar conditions. Toluene was used as the radical scavenger with a 50-fold excess of nitric oxide in one run (filled squares) and a 100-fold excess in the other (unfilled squares). As shown in Table II, the Arrhenius parameters for the dimethylnitramine decomposition in the presence of excess NO, with either toluene or cyclopentane as the radical scavenger, are essentially the same, i.e., log $k$ (s$^{-1}$) = 13.5 ± 0.6 − (37.4 ± 2.5)/2.3$RT$.

Data obtained with toluene as the scavenger and in the absence of nitric oxide are also plotted in Figure 2. In this case no more than 60% of the decomposed dimethylnitramine could be accounted for, appearing as dimethylnitrosamine (25%), methylmethylenimine (~20%), nitrous acid (~12%), dimethylamine (~8%), and *N,N*-dimethylbenzylamine (~3). These yields varied with temperature, with the dimethylnitrosamine yield being smaller at the lower end of the temperature range. Trace amounts of *N,N*-dimethylacetamide were tentatively identified. Unlike runs with excess NO, in which virtually identical comparative rate plots are obtained from either reactant disappearance or product appearance, the comparative rate plot for data obtained in the absence of excess NO could only be based on the amount of dimethylnitramine lost. Nevertheless, as shown in Figure 2 and in Table II, the Arrhenius parameters obtained for dimethylnitramine decomposition in the absence of excess nitric oxide are still similar to those obtained in its presence.

Prior to the use of HMP as the temperature standard in the thermal decomposition of dimethylnitramine, *tert*-butyl bromide was used as the temperature standard[11] in several runs in which the nature of the radical scavenger or of the nitrogen oxide present in the gas mixture was varied. The Arrhenius parameters obtained from the resulting comparative rate plots were similar to those obtained with HMP. However, due to experimental difficulties (see Experimental Section), attempted mass balances for both the temperature standard and the dimethylnitramine ranged widely. The quantitative results were therefore considered unreliable and are not reported here (even though the Arrhenius parameters generally fall within the range shown in Table II). The following qualitative observations from these runs are nonetheless considered pertinent in understanding this system's complexities, and we attempted to incorporate them in the mechanistic modeling of the DMNA decomposition.

In the absence of excess nitrogen oxides, use of toluene as a radical scavenger resulted in the formation of *N,N*-dimethylbenzylamine, benzene, and bibenzyl in addition to the formation of *N,N*-dimethylnitrosamine as the major product and formaldehyde in trace amounts. Use of cyclopentane as the radical scavenger gave, in addition to nitrosamine and formaldehyde, nitrocyclopentane and cyclopentene.

Since the reduction of $NO_2$ in secondary reactions is considered to be a critical step in dimethylnitrosamine production via recombination of the dimethylamino radical with NO, dimethylnitramine decomposition was also studied in the presence of toluene, *tert*-butyl bromide, and roughly a 100-fold excess of nitrogen dioxide. Although a temperature standard was not included in this run, excess $NO_2$ appeared to have no substantial effect on the dimethylnitramine decomposition rate.

When the dimethylnitramine decomposition was carried out in the absence of radical scavenger or of nitrogen oxides, dimethylnitrosamine continued to be the major product, but formaldehyde was produced in more than 50% yield (relative to nitrosamine produced), and the rate of nitramine loss apparently increased by a factor of from 2 to 5. (The exact extent of acceleration is uncertain because the temperature standard was also absent in these runs.)

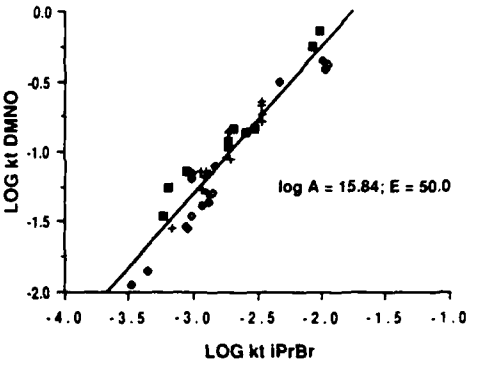


**Figure 3.** Comparative rate plot of dimethylnitrosamine (DMNO) vs isopropyl bromide (*i*-PrBr). (The different symbols represent experiments on different days.)

In order to check the behavior of our temperature standard, HMP, its Arrhenius parameters were independently determined by using the LPHP comparative rate technique with *t*-butyl bromide as the temperature standard (literature parameters[11] log $k$/s$^{-1}$ = 13.8 − 41.8/2.3$RT$). The $A$ factor and activation energy for HMP thus determined were in excellent agreement with those reported in the literature[10] (log $A$ = 11.9 vs 11.6 and $E_a$ = 32.9 vs 32.8 kcal/mol, respectively). This result, along with the good mass balances obtained for dimethylnitramine decomposition in the presence of excess nitric oxide and the similar Arrhenius parameters found for dimethylnitramine with *tert*-butyl bromide as the temperature standard, all suggest that the Arrhenius parameters we report for dimethylnitramine are not distorted by systematic errors resulting from different temperature tracking behaviors.

Because of its importance as a product, the thermal decomposition of dimethylnitrosamine was also studied over the temperature range 870–990 K, with isopropyl bromide as the temperature standard. The comparative rate plot is shown in Figure 3. With dimethylnitrosamine the sequence of secondary gas-phase reactions is considerably simpler than with dimethylnitramine since the formation of imine by loss of a hydrogen atom is, in the presence of scavenger, essentially irreversible, and the sequence of oxidation steps that takes place when $NO_2$ is present cannot occur here. However, GC analysis of the imine presents a problem, since the proclivity of imines for polymerization reactions means that any surface contacted by the imine (e.g., in the heated transfer lines) is a candidate for promoting polymerization. The extent of this polymerization varies from day to day, exhibiting a sensitivity to factors not easily defined. Samples of the gummy polymer were collected and subjected to analysis by field ionization mass spectrometry (FIMS). The dominant peak in the pyrolysis/FIMS spectra of this material was $m/z$ 86, corresponding to an imine dimer produced from thermal decomposition of the imine polymer.

The net result of this behavior is that, although the gas-phase secondary reactions of dimethylnitrosamine are much simpler than for dimethylnitramine, reliable quantitative product analysis is very difficult. Hence, the kinetics were based solely on DMNO disappearance, and there is substantial scatter in the comparative rate plot. This scatter notwithstanding, the parameters extracted from the data in Figure 3 are consistent both with the expectation of simple N–NO bond scission as the rate-limiting step and with the BAC-4 calculations of Melius[12] that suggest N–NO bonds

(11) Tsang, W. *J. Chem. Phys.* **1964**, *40*, 1498.

(12) Melius, C. F.; Binkley, J. S. In *Proceedings of the 21st Symposium (International) on Combustion*, 1987; The Combustion Institute: Pittsburgh, PA, 1988; p 1953.

**TABLE III: Parameters Used in Numerical Modeling of Dimethylnitramine and Dimethylnitrosamine Decomposition**

| no. | reaction | log $A^a$ | $E_a$, kcal/mol |
|---|---|---|---|
| 1 | $(CH_3)_2N-NO_2 \rightarrow (CH_3)_2N + NO_2$ | 15.3 | 46.5 |
| 2 | $(CH_3)_2N-NO_2 \leftarrow (CH_3)_2N + NO_2$ | 8.8 | -2.0 |
| 3 | $(CH_3)_2N-NO_2 \rightarrow (CH_3)_2N-O-N=O$ | 11.5 | 31.0 |
| 4 | $(CH_3)_2N-NO_2 \leftarrow (CH_3)_2N-O-N=O$ | 10.5 | 11.1 |
| 5 | $(CH_3)_2N-ON=O \rightarrow (CH_3)_2N-O^{\bullet} + NO$ | 13.7 | 9.0 |
| 6 | $(CH_3)_2N-O-N=O \leftarrow (CH_3)_2N-O^{\bullet} + NO$ | 9.9 | 0.0 |
| 7 | $(CH_3)_2N^{\bullet} + NO_2 \rightarrow (CH_3)_2N-O^{\bullet} + NO$ | 10.0 | 0.0 |
| 8 | $(CH_3)_2N^{\bullet} + NO_2 \leftarrow (CH_3)_2N-O^{\bullet} + NO$ | 9.9 | 13.8 |
| 9 | $(CH_3)_2N^{\bullet} + NO \rightarrow (CH_3)_2N-NO$ | 9.8 | -2.0 |
| 10 | $(CH_3)_2N^{\bullet} + NO \leftarrow (CH_3)_2N-NO$ | 15.5 | 50.3 |
| 11 | $(CH_3)_2N-O-N=O + NO \rightarrow (CH_3)_2N-NO + NO_2$ | 9.7 | 5.0 |
| 12 | $(CH_3)_2N-NO_2 + H^{\bullet} \rightarrow (CH_3)_2N-NO + OH^{\bullet}$ | 10.0 | 0.0 |
| 13 | $(CH_3)_2N-NO_2 + CH_3^{\bullet} \rightarrow (CH_3)_2N-NO + CH_3O$ | 9.0 | 0.0 |

[a] Units of $A$ are $s^{-1}$ and L/(m s) for unimolecular and bimolecular reactions, respectively.

DMNA DECOMPOSITION MECHANISM

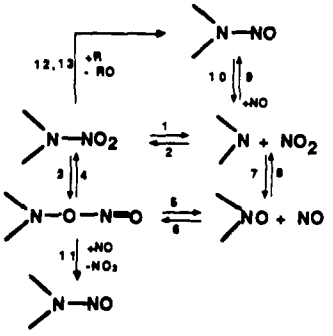


**Figure 4.** Schematic representation of the mechanism at DMNA decomposition in the presence of excess NO.

are *not* weaker than their N–$NO_2$ counterparts, in marked contrast to C–NO bonds and their C–$NO_2$ counterparts.[13] Thus, this result serves to reiterate that the LPHP technique behaves as claimed and impels us to examine the chemistry more closely in the case of dimethylnitramine.

*Numerical Modeling.* In considering the data presented above, the goal was to choose a sequence of reactions that (1) explained the observed products and the relative yield in which they are formed, (2) explained the observed overall rate parameters, and (3) did so with known or plausible parameters for each of the elementary processes. The mechanistic numerical model we constructed to help explain the results (decomposition of dimethylnitramine) consists of 75 primary and secondary reactions that account for all of the observed products. Reverse reactions were initially included for all reactions; some were dropped from the model when thermochemically limited parameters and numerical integration showed them to be of negligible importance. Certain reactions postulated in the literature as important contributors for the dimethylnitramine decompostion were retained in the model even if thermochemical limitations ruled out their importance.

The Arrhenius parameters for all reactions were taken from the literature where possible; otherwise, they were derived by estimation teqhniques from analogous reactions in the literature. Where appropriate, the degree of falloff was estimated by the RRK method. Instead of discussing each reaction and the parameters used for it individually, the main reactions in the model are schematically depicted in Figure 4. In Table III we list the rate parameters for the reactions included in Figure 4. We have

(13) McMillen, D. F.; Golden, D. M. *Annu. Rev. Phys. Chem.* **1982**, *33*, 497.

(14) See, for example: Kerr, J. A.; Moss, S. J. *CRC Handbook of Bimolecular and Termolecular Gas Reactions*; CRC Press: Boca Raton, FL, 1981; Vols. 1 and 2. Tsang, W.; Hampson, *J. Phys. Chem. Ref. Data* **1986**, *15*, 1087–1279.

MODEL RESULTS

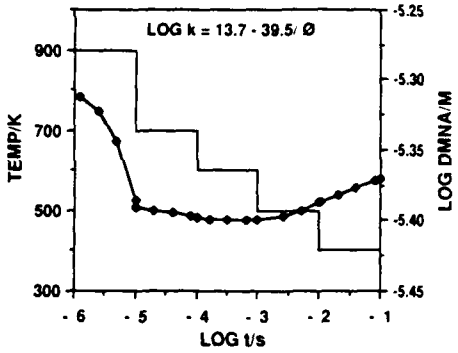


**Figure 5.** Schematic representation of the temperatures changes with time imposed during numerical modeling to represent LPHP conditions. Also shown is the computed variation of DMNA with time. Initial conditions for model: cell temperature 367 °C, $P_0$(DMNA) = 0.11 Torr, $P_0$(*o*-fluorotoluene), $P_0$(NO) = 5.7 Torr, $P_0$(hydroxymethylpentanone) = 0.11 Torr.

endeavored to assure maximum utility for the modeling effort by remaining cognizant of the fact that literature data[14] for all of the reaction types allow only a limited range within which the parameters can be varied without pressing the limits of plausibility.

In order to approximate the physical characteristics of the LPHP system and to account for the possibility of reaction during cooling (primarily low activation energy secondary reactions of radicals) of the laser-heated portion of the cell, the model incorporated a drop of 200 K (from the initial 900 K) at the end of the first time decade (10 μs), followed by 100 K drops at the end of each succeeding decade. The sequence of differential equations provided by the reactions was then integrated over time and temperature by a program that uses a numerical integration routine based on the Gear algorithm. The temperature profile and the computed dimethylnitramine concentration as a function of time are shown in Figure 5.

The experimental temperature dependence and product yields under different conditions were successfully reproduced only when the model included the nitro–nitrite rearrangement and also reactions 4, 6, and 11. These reactions are reversal of the nitro–nitrite rearrangement, reversal of the nitrite thermolysis, and displacement of $NO_2$ from the nitrite by NO, respectively. The reasonableness of these reactions is considered in the following section; taken at face value, the computed values suggest that the experimental results do in fact reflect initial competition between simple bond scission and nitro–nitrite rearrangement, each with the parameters shown in Table III.

## Discussion

As described in the preceding section, the mechanism whose important elements are shown in Figure 4 is able to reproduce the data, including nitramine decomposition rate parameters and dimethylnitrosamine yield under a range of experimental conditions, and furthermore does so with rate parameters for the various steps that are either experimentally determined or plausible extrapolations from related reactions. In this section, we examine the key steps in the model and discuss them relative to those that have been suggested in previous studies to account for observed rates and products.

The basic experimental results that must be duplicated if a dimethylnitramine decomposition mechanism is to be considered potentially valid are the decomposition rate and dimethylnitrosamine yield as a function of temperature and radical scavenger/trap concentrations. The difficulty that this seemingly simple requirement presents is that the experimental parameters are too low for simple bond scission to be the dominant rate-determining step, but any molecular elimination or rearrangement pathway that one writes to allow duplication of the Arrhenius parameters does not lead, by a simple sequence of known reactions, to the observed dimethylnitrosamine yields. Specifically, such sequences do not provide a route from the nitroxyl radical (which is the

unavoidable scission product that follows nitro–nitrite rearrangement) to the nitrosamine. (One might have imagined that HONO from molecular elimination could take part in some surface-promoted nitrosation of amine during transport of the reaction products to the GC–MS system, but this would have involved reaction with the amine rather than the imine. Furthermore, the imine tends to undergo a variable amount of polymerization on the walls of the transfer lines; the observed yield of dimethylnitrosamine is quite reproducible and therefore not easily connected with reactions subject to variations in surface conditions.)

Given the notorious susceptibility of even precisely measured Arrhenius parameters to distortion by systematic error, we were initially inclined to assign the low-temperature dependence to such distortions and conclude that the 100% yield of nitrosamine produced in the presence of excess NO simply resulted from trapping a quantitative yield of dimethylamino radicals produced in an initial $N–NO_2$ bond scission. However, the rate measurements made under a wide range of experimental conditions that were employed in an effort to minimize distortion of the temperature dependence by spurious secondary reactions have repeatedly given $\log k\ (s^{-1}) = 13.5 \pm 0.6 - (37.4 \pm 2.5)/2.3RT$, as described in the preceding section. Furthermore, we conclude that there is no significant distortion of the temperature dependence by the highly reactive imine, since pyrolysis of dimethylnitrosamine, which yields the imine as the dominant product, produces a temperature dependence completely consistent with an N–NO bond scission. [Finally, preliminary results of dimethylnitramine pyrolysis in a molecular beam mass spectrometrically sampled LPHP cell reveal that mass 60 and mass 30 (presumably dimethylnitroxyl radical and NO) are products of an initial unimolecular decomposition step.] Thus, the results indicating that a low $A$ factor initial step contributes to dimethylnitramine decomposition became too consistent to simply reject out of hand and demanded a plausible mechanism that could account for them.

The critical reactions that make it possible for the numerical model to duplicate the low Arrhenius parameters and high dimethylnitrosamine yields in the presence of excess NO are shown in Figure 4 and Table III, which have been abridged for purposes of discussion. The critical elements are the following:

1. $N–NO_2$ bond scission and $NO_2$–ONO rearrangement that are roughly competitive at 900 K (reactions 1 and 3).
2. Rapid, but *reversible*, thermolysis of the very weak O–NO bond in the *N*-nitrite (reactions 5 and 6).
3. Reverse of the nitro–nitrite rearrangement (reaction 4).
4. Attack of NO on the *N*-nitrite to displace $NO_2$ and yield directly the nitrosamine (reaction 11).

The reverse reactions of the nitro–nitrite rearrangement and of the nitrite thermolysis are required by microscopic reversibility (though we did not initially anticipate their impact). Reversal of the O–NO bond thermolysis is important only in the presence of excess NO, and it is only this reversal that can maintain a high enough steady-state concentration of the weakly bonded nitrite such that reversal of the nitro–nitrite rearrangement (reaction 4) becomes significant. It is this latter reaction that allows some return to the nitramine and helps to limit the formation, under these conditions, of other products from the nitroxyl radical.

The only reaction in the sequence without direct precedent is reaction 11, the displacement of $NO_2$ from the nitrite by NO. This reaction is most important at lower temperatures. Because it is a low activation energy process and it limits return from the nitrite, it serves to substantially increase the net decomposition at low temperatures, while providing an additional route to nitrosamine. As an addition–elimination reaction between a free radical and a substrate having partial double-bond character, it is the type of reaction that could well proceed with a low activation energy. As currently incorporated in the model, it has a 5 kcal/mol activation energy. If this is raised to 10 kcal/mol, the computed overall activation energy for DMNA loss is raised from 39.5 to 44.5 kcal/mol (i.e., 75% of the way to the 46.1 kcal/mol that results from complete elimination of reaction 11). There may conceivably be alternatives to reaction 11; as the reaction sequence is currently written, this reaction constitutes a necessary and reasonable route to nitrosamine from the easily formed nitroxyl radical. That is, if nitrosamine is to be formed from the nitroxyl radical, the oxygen on the nitrogen clearly must depart, and departing as one of the oxygens on an $NO_2$ seems an eminently reasonable way to accomplish this. It is interesting to note that the stability of the nitroxyl radical at the same time makes it the inevitable product of the nitro–nitrite rearrangement and a bottleneck in the further decomposition of the amine framework. This bottleneck, in turn, is what evidently makes it possible for a major ultimate product of the nitro–nitrite rearrangement to be the nitrosamine.

In this and the following paragraphs, we consider some of the other reactions that have been previously suggested for nitrosamine formation. Beginning with the results of Fluornoy[1] some years ago, a number of suggestions have been made for the formation of dimethylnitrosamine as the main product from the thermal decomposition of dimethylnitramine. Two of these, namely unimolecular oxygen atom loss (15) and NO addition to the imine followed by scavenging of the resulting carbon-centered radical (16), can be ruled out on thermochemical grounds. Reaction

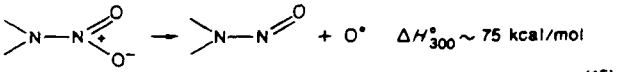


(15)

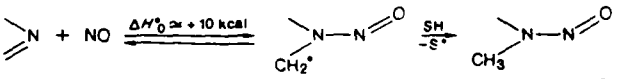


(16)

15 is not a possible explanation because it has an endothermicity[12] substantially exceeding the observed activation energy for nitrosamine production. Reaction 16 is unfavorable because the exothermic decomposition of the intermediate (reaction −16) is much faster than it stabilization by any conceivable[13] scavenger.

The remaining candidates that need to be considered include recombination of NO with the dimethylamino radical (9) as invoked by Lin,[2] radical addition to one of the nitro group oxygens as discussed by Melius[12] (12, 13) (i.e., direct biomolecular reduction of the intact nitramine), and bimolecular or unimolecular formation of the unstable *O*-nitroso compound (6, 3) as an effective route to high yields of NO to serve as an intermediate for reaction 9.

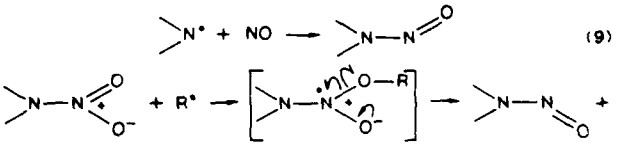


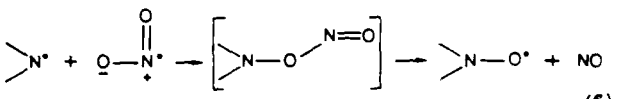


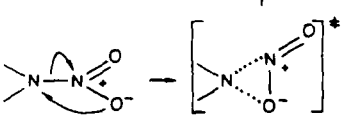


The recombination of NO with the dimethylamino radical is the logical first candidate and has been invoked by all previous workers as a major source of nitrosamine; this step can be preceded by NO production routes consisting of a sequence of "known" unimolecular and bimolecular reactions (1 and 7) and/or by the nitro–nitrite rearrangement (3) which has precedent as a unimolecular process in nitromethane[15] and nitrobenzene[16,17] de-

(15) Wodtke, A. M.; Hintsa, E. J.; Lee, Y. T. *J. Phys. Chem.* **1986**, *90*, 3549.
(16) Gonzalez, A. C.; Larson, C. W.; McMillen, D. F.; Golden, D. M. *J. Phys. Chem.* **1985**, *89*, 4809.

composition.

The four-center "recombination" leading directly to two nitrosomethane molecules suggested by Lin would appear to have steric requirements that are too stringent to be the high $A$ factor process that is evidently required to explain his observations. On the other hand, reaction 17 is not an unreasonable suggestion on enthalpic grounds, given the known tendency[18] of $C$-nitroso compounds to dimerize.

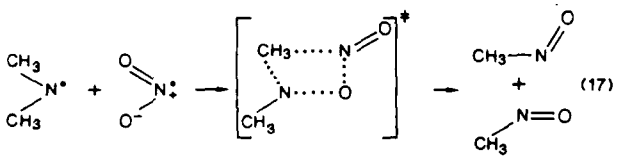

(17)

The model used by Lin successfully reproduced his observed DMNA decomposition and DMNO formation rates through a route involving almost complete oxidative fragmentation of the amino structure and formation of NO as an intermediate in rather large yields in the process. However, there are several key steps whose parameters need to be carefully assessed in order to judge the adequacy of the reaction scheme as assembled by Lin. These are the four-center recombination (17) considered above, the oxidation of the dimethylamino radical by $NO_2$ (7), and the thermolysis of nitrosomethane.

Reaction 17 can be viewed as a disproportionation with rather severe steric requirements. While the impact of these requirements on the rate may be tempered by the fact that the nitrosomethane dimer is bound[18] by about 17 kcal/mol, an $A$ factor of $3 \times 10^9$ L/(m s) is still surprisingly high. Furthermore, for this reaction to take place to the exclusion of the recombination at an oxygen atom site (i.e., reaction 7), a known reaction that has no unusual steric requirements and leads to oxidation of the radical, is even more surprising. In principle, this "known" route can lead to the same products as the four-center recombination (17), since oxidation of the dimethylamino radical gives a nitroxyl radical (7), which upon $\beta$-scission, gives the methyl radical and a molecule of nitrosomethane.

$$(CH_3)_2N\text{–}O^{\bullet} \rightarrow CH_3NO + CH_3^{\bullet} \qquad (18)$$

Thermolysis of nitrosomethane then gives NO and another methyl radical, which can go on to reduce more $NO_2$ to NO.

$$CH_3\text{–}NO \rightarrow CH_3^{\bullet} + NO \qquad (19)$$

Whether the sequence of reactions 7, 18, and 19 will in practice give the same results as reactions 17 and 19 is another question, since nitroxyl radicals are quite stable in general, and this particular one is estimated[12] to have a methyl–N bond strength of 44 kcal/mol.

Finally, the unimolecular dissocation (19) of the nitrosomethane itself is another step at which a bottleneck must be avoided, if recombination as the sole route to nitrosomethane is to satisfactorily explain the various experimental results. The parameters that Lin[2] has evidently found necessary for this step to be fast enough include an $A$ factor of $5 \times 10^{16}$ L/(m s). Values in the literature[14] for loss of diatomic fragments, as well as consideration of the overall entropy change in this particular reaction, indicate that $5 \times 10^{16}$ is about an order of magnitude too large for nitrosomethane thermolysis, without consideration of the effects of falloff. In fact, use of all the other parameters chosen by Lin, but with the $A$ factor for this reaction lowered to $5 \times 10^{15}$, lowered the computed dimethylnitrosamine yield at 500 K from the observed 60% to 40%. These difficulties do not absolutely rule out NO recombination as the sole route to the nitrosamine but serve at least to (a) quantify the intuition that a delicate balance among secondary reactions is required in order to produce enough NO for nitrosamine production through recombination, while still leaving enough intact dimethylamino radicals to recombine with the NO, and (b) amplify Lin's original finding that a fully satisfactory explanation does not easily follow from previously documented reactions.

A nitrosamine formation route that would not require a critical balance between amino radical survival and oxidative fragmentation is the one first made by Schroeder[19] and recently subjected by Melius[12] to calculation by the BAC-MP4 method. If reaction 12 is facile enough, it will result in rapid formation of the nitrosamine from virtually any radical produced in the system.

Reactions 12 and 13 are quite reasonable: they are molecular analogues to the oxidation of radicals by $NO_2$. Since they are not radical–radical reactions, but radical additions to a double bond, one might expect them to exhibit activation energies types of those classes of reactions (1–2 kcal/mol for H atoms and 5–7 kcal/mol for carbon-centered radicals). However, the calculation of Melius[12] evidently suggest little or no activation energy for methyl radicals as well as for hydrogen atoms. Thus, in order to derive an upper limit to the possible importance of these reactions, we have incorporated them (for R = $H^{\bullet}$ and $CH_3^{\bullet}$) into the numerical model described above using appropriate $A$ factors and zero activation energies for methyl radicals as well as hydrogen atoms. Under these conditions, the computation showed that reaction under the modeled temperature–time history illustrated in Figure 5 and in the presence of a 50-fold excess of toluene as radical scavenger resulted in a contribution to dimethylnitrosamine production from reactions 12 and 13 that was no more than 20% of the total yield of that product. Furthermore, the inclusion of these reactions did not lead to a tendency toward lower Arrhenius parameters. Thus, while they may be important during actual nitramine combustion, the nitrosamine formation reactions considered by Melius[12] would seem not to be responsible for the low $A$ factors and low activation energies observed under our scavenged laser pyrolysis conditions. In other words, we cannot, by inclusion of these reactions in the model, duplicate the observed temperature dependence for DNMA loss, namely, an $A$ factor and activation energy 2 powers of 10 and 10 kcal/mol, respectively, below those indicative of simple N–$NO_2$ bond scission.

## Summary

The decomposition temperature dependence and the product yields in the laser pyrolysis of dimethylnitramine can be accounted for (1) by a combination of competing unimolecular bond scission and nitro–nitrite rearrangement as the initial loss reactions and (2) by a low-temperature pathway to nitrosamine that involves reversals of the nitro–nitrite rearrangement and nitrite homolysis steps, coupled with a direct route from the unstable nitrite (or its oxidation-state equivalent, the nitroxyl radical) to dimethylnitrosamine. Among these, the latter is the only reaction strictly without precedent; even it, as a displacement of $NO_2$ from the nitrite by NO, is somewhat analogous to radical addition to a double bond. Parameters assigned to it on this basis allow the experimental observations to be reproduced without abandoning plausibility.

These results reveal competing initial reactions and facile secondary reactions in the decomposition of a simple nitramine. Understanding the range of possible reactions is clearly a necessary part of understanding the conditions required for the decomposition of this and more complex nitramines to become thermally self-sustaining. It is entirely fitting that our attempt to further this understanding is presented as part of a tribute to Fred Kaufman, who so aptly described endeavors such as this in his seminal plenary lecture[20] to the 19th Symposium (International) on Combustion. Experiments now under way with a different LPHP apparatus, in which the initial products of laser decomposition are detected directly via molecular beam mass spectrometry, will provide ad-

(17) Tsang, W.; Robaugh, D.; Mallard, W. G. *J. Phys. Chem.* **1986**, *90*, 5968.

(18) Batt, L.; Robinson, G. N. In *Chemistry of Functional Groups: Supplement F*; Patai, S., Ed.; Wiley: Chichester, 1981; p 1035.

(19) Schroeder, M. A. In *Proceedings of the 16th JANNAF Combustion Meeting*; CPIa: 1978; Vol. *82*, p 644. 1979; Vol. 2, p 17.

(20) Kaufman, F. In *Proceedings of the 19th Symposium (International) on Combustion 1981*; The Combustion Institute: Pittsburgh, PA, 1982; p 1.

ditional information about this competition.

*Acknowledgment.* We acknowledge the support of the U.S. Army Research Office under Contract DAAC03-86-K-0030 and the Air Force Office of Scientific Research under Contract F49620-85-K-00006. We also thank Alicia C. Gonzalez for experimental efforts in the early part of this work. D.M.G. acknowledges the joy of having worked with and been a friend of Fred Kaufman. His enthusiasm, humor, and essential humanity are sorely missed.

**Registry No.** DMNA, 4164-28-7; DMNO, 62-75-9; toluene, 108-88-3; methylmethylenimine, 1761-67-7; dimethylamine, 124-40-3; *N,N*-dimethylbenzylamine, 103-83-3.

# Appendix B

# MOLECULAR-BEAM SAMPLED LASER PYROLYSIS OF DIMETHYLNITRAMINE

Reprinted from The Journal of Physical Chemistry, 1989, 93, 3557.


# Molecular Beam Sampled Laser Pyrolysis of Dimethylnitramine

**Paul H. Stewart,[†] Jay B. Jeffries, Jean-Michel Zellweger,[‡] Donald F. McMillen,* and David M. Golden**

*Department of Chemical Kinetics, Chemical Physics Laboratory, SRI International, Menlo Park, California 94025* *(Received: May 9, 1988; In Final Form: November 8, 1988)*

A pulsed $CO_2$ laser was used to create a thermally heated volume within a mixture of argon, $SF_6$, and dimethylnitramine (DMNA) in a flow cell, such that the periphery of the laser-heated region was immediately adjacent to a molecular beam/quadrupole mass spectrometer sampling system. Detection of the product mixture in the molecular beam revealed that initial N–$NO_2$ scission was accompanied by a comparable amount of the nitro–nitrite rearrangement (followed by rapid scission of the extremely weak $(CH_3)_2NO$–NO bond) to produce directly NO and the nitroxyl radical. Production of this NO by secondary bimolecular reactions can be ruled out because the time available before the product mixture was frozen by expansion was too short and because the observed rise times of the NO and $NO_2$ were identical. Calibration of the detection system with laser-heated NO and $NO_2$ at the reaction temperature (900 ± 50 K) revealed that the rearrangement/bond-scission branching ratio is ~0.7:1.0. These results raise questions about previous studies of dimethylnitramine concluding that N–$NO_2$ bond scission is the sole rate-limiting step and suggest that "loose" nitro–nitrite rearrangements may be a general phenomenon in N–nitro compounds, as they appear to be in C–nitro compounds.

## Introduction

The initial decomposition step(s) of nitramines have been of interest for some time as one of the important keys to understanding what controls the initiation and combustion of nitramine explosives and propellants, respectively. For any energetic material this information tends to be difficult to obtain, since the utility of such materials is based on their tendency to undergo extremely rapid and exothermic decomposition once certain kinetic bottlenecks have been passed, thus obscuring the identity of the bottleneck reaction (or reactions). Furthermore, as has been appreciated for some time, the functionally useful nitramines have a multiplicity of candidate initial steps that can be identified on the basis of existing thermochemical information; however, this information is not sufficiently precise or reliable to allow an a priori distinction among the various candidates. Finally, the situation is further aggravated because secondary bimolecular reactions of radicals with $NO_2$ are known to be extremely fast and can be expected to complicate attempts to disentangle the reaction sequence.

For all of the above reasons, dimethylnitramine (DMNA) has been studied by various workers as a simple analogue expected to exhibit some of the reactions that are important for the cyclic nitramines. However, the apparent simplicity of DMNA notwithstanding, it has been dificult to determine with certainty the initial decomposition step(s). Original work by Fluornoy[1] and by Korsunskii and co-workers[2] identified N–$NO_2$ bond scission as the initial step, although this was a matter of assignment rather than demonstration, as the temperature dependence of the initial step was obscured to an uncertain degree by secondary reactions. More recently, Lin and co-workers[3] reported low-temperature

[†] Postdoctoral Research Associate.
[‡] Present address: CIBA-GEIGY, CH-4333 Munchwillen/AG, Schweiz, Switzerland.

(1) Fluornoy, J. M. *J. Chem. Phys.* **1962**, *36*, 1106.
(2) (a) Korsunskii, B. L.; Dubovitskii, F. I.; Sitonian, G. V. *Dokl. Akad. Nauk SSSR* **1967**, *174*(5), 1126. (b) Korsunskii, B. L.; Dubovitskii, F. I. *Dokl. Akad. Nauk SSSR* **1964**, *155*(2), 402.

0022-3654/89/2093-3557$01.50/0 

static bulb experiments and high-temperature single-pulse shock-tube results, which when coupled together give an activation energy, measured over a wide temperature range, that is indicative of initial N-$NO_2$ bond scission. Similarly, Wodtke and Lee[4] have made preliminary reports of infrared multiphoton decomposition in a molecular beam also leading to the tentative conclusion that N-$NO_2$ is the exclusive (i.e., ≥95%) initial reaction. In contrast with these results, comparative rate GC-analyzed laser pyrolysis experiments in this laboratory repeatedly gave a temperature dependence for DMNA decomposition that is not consistent with initial N-$NO_2$ bond scission.[6]

A choice between those results supporting and those contravening N-$NO_2$ bond scission as the sole rate-limiting step cannot be made without reservations. The shock-tube and static-bulb work[1-3] were performed without radical scavengers, and there is therefore no assurance that the decomposition rates are not perturbed by secondary reactions. In particular, for single-pulse shock-tube kinetic studies of hydrocarbon decomposition, there is a general need for scavengers to inhibit hydrogen atom chain reactions, when those are structurally possible. On the other hand, the finding, in the GC/MS-monitored laser pyrolysis studies, of an $A$ factor (and an activation energy) too low to be consistent with rate-limiting unimolecular based scission hardly constitutes ironclad evidence, given the notorious susceptibility of Arrhenius parameters to distortion by systematic errors. The multiphoton decomposition of DMNA in a molecular beam, where there can be no ambiguity about secondary bimolecular reactions, has thus far been presented only in preliminary form. Furthermore, the average energy input to reacting DMNA molecules may have been much higher than that which is obtained at thermal bath temperatures of 400–700 °C.

The literature data outlined above, its limitations notwithstanding, together with our own previous experience with dimethylnitramine,[5] led us to expect that N-$NO_2$ bond scission would be the dominant, and perhaps exclusive, reaction at 900 K. Thus, when we repeatedly obtained, in GC-monitored laser pyrolysis experiments,[6] a temperature dependence indicative of a contribution from a low $A$ factor process, we responded by changing reaction conditions in search of a suspected systematic error. When these efforts, which involved varying the partial pressures and identities of the radical scavengers and the temperature standard, and the use of NO as a radical trap, all still resulted in a temperature dependence too low to indicate N-$NO_2$ as the sole rate-determining step, we concluded that direct observation of the initial step(s) was indicated. In this paper, we describe the molecular beam sampled, mass spectrometric detection of the initial products from the $SF_6$-sensitized laser pyrolysis of dimethylnitramine.

## Experimental Procedure

The thermal decomposition of dimethylnitramine was studied by using a laser-powered homogeneous pyrolysis system coupled with a molecular beam/mass spectrometer detection system. The results for DMNA are the first with this new apparatus, and the experimental technique is presented in detail. A pulsed $CO_2$ laser was used to irradiate a flowing mixture of sulfur hexafluoride ($SF_6$ at 3 Torr) absorber molecules, argon bath gas (≥36 Torr), and DMNA (ca. 0.5 Torr) substrate. Following collisional energy transfer, the heated DMNA thermally decomposed. A molecular beam of the heated gas was formed by expansion through a 75-μm-diameter nozzle. The partial pressures are such that the heated DMNA undergoes more than 10000 collisions before it decomposes. Similarly, the partial pressures and fractional decomposition are such that initially produced $NO_2$ will experience 1000–10000 collisions with Ar or $SF_6$ for every possible reactive collision with a dimethylamino radical. Thus, the conditions should favor thermalization of the reactants but allow beam formation before substantial secondary bimolecular reaction can take place. As noted below, when the DMNA concentration is increased and the temperature is increased to cause ~60% decomposition, secondary reaction of the $NO_2$ is clearly observed. The data presented here are taken at conditions where we observe no evidence of secondary reactions. The beam was analyzed by means of a quadrupole mass spectrometer (QMS), which allowed the direct detection of initial reaction products.

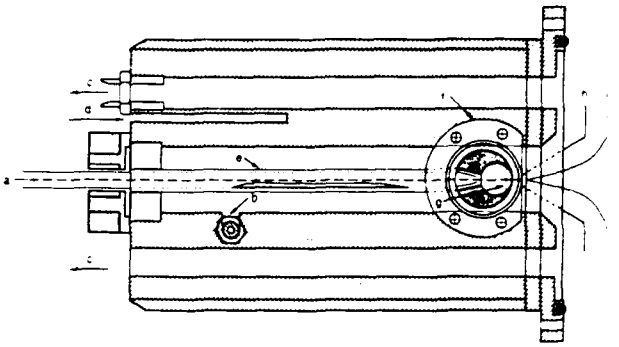

**Figure 1.** Schematic drawing of the machined aluminum flow cell: (a) carrier gas inlet, (b) dilution gas inlet, (c) flow cell pump-out, (d) well for thermocouple, (e) substrate reservoir, (f) retaining ring and shroud for KCl windows, (g) location of nozzle, (h) nozzle support, (i) skimmer.

*Flow System.* The reaction mixture was prepared by establishing a flow of a commercially prepared 10% $SF_6$/argon mixture (Matheson) through a glass tube containing the DMNA. The total pressure was maintained at a constant level (30–90 Torr) by using a pressure regulator and controlling the pump-out rate of the cell. The "reservoir" tube containing the DMNA extended into the heated flow cell through an O-ring-sealed Cajon fitting (Figure 1). In this manner, controlled amounts of the nitramine vapor were introduced into the flow. The end of the glass reservoir was positioned as close to the laser-heated region as possible (to minimize surface effects). The aluminum reaction cell was maintained at a temperature typically in the range 25–35 °C. The gas mixture was irradiated through the KCl windows at 2.0 Hz by a pulsed 10.6-μm $CO_2$-laser beam of energy ≤1.8 J/$cm^2$ and 1-μs duration. A mechanical pump was used to control the gas flow at a rate that ensured complete renewal of the reaction mixture between laser pulses (0.5 s). The laser-heated region was cylindrical in shape, 1.1 cm in diameter, and 2.5 cm long. The laser beam was positioned to irradiate the reaction mixture as close as possible (≤1 mm) to the nozzle, so that the expansion wave generated by the laser heating pushed the gas inside the nozzle. Thus, a few microseconds after the laser pulse, the leading edge of the laser-heated region has expanded into the orifice, whereupon molecular beam formation freezes the composition. The cooling rate during adiabatic expansion itself is greater than $10^6$ °C/s. However, the rapid initial temperature drop is only 100–200 °C, enough to shut off high activation energy (i.e., thermolysis) reactions but not enough to stop rapid bimolecular reactions (e.g., H-atom abstractions, additions, $NO_2$ oxidations of radicals), some of which may even have a small negative temperature dependence. These reactions are not stopped until beam formation eliminates further collisions. Whatever radicals are formed in the initial decomposition steps and persist until the orifice is reached are then transported without undergoing further collision to the QMS in less than a millisecond.

*Beam-Sampling System.* The supersonic divergent nozzle consisted of a platinum disk (0.80 cm in diameter and 100 μm thick) with a 75-μm-diameter hole at its center (Ernest F. Fullam, Inc., Latham, NY). This disk was positioned at the apex of a conical support and held firmly in place by a screw cap. A skimmer (electroformed nickel, Beam Dynamics, Minneapolis, MN) with a 200-μm diameter at the throat extracted the central

(3) (a) Lloyd, S. A.; Umstead, M. E.; Lin M. C. *J. Energ. Mater.* **1985**, *3*, 187. (b) Umstead, M. E.; Lloyd, S. A.; Lin, M. C. *Proc. 22nd JANNAF Combust. Mtg., CPIA* **1985**, 512.

(4) Wodtke, A. M., private communication.

(5) McMillen, D. F.; Barker, J. R.; Lewis, K. E.; Trevor, P. L.; Golden, D. M. "Mechanisms of Nitramine Decomposition: Very Low-Pressure Pyrolysis of HMX and Dimethylnitramine"; Final Report, SRI Project PYU-5787, 18 June 1979 (SAN 0115/117). DOE Contract No. EY-76-C-03-0115.

(6) Nigenda, S. E.; McMillen, D. F.; Golden, D. M., submitted for publication in *J. Phys. Chem.*

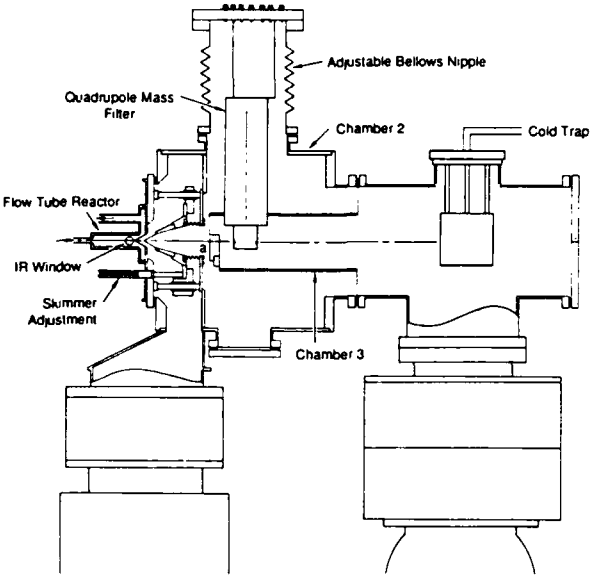


**Figure 2.** Schematic drawing of the molecular beam sampled, mass spectrometrically detected LPHP system. For the sake of clarity, the diffusion pump associated with chamber 2 has been omitted (a, chopper).

portion of the beam. The distance between the nozzle and the skimmer entrance could be varied from a few millimeters up to 20 mm by external adjustment of a micrometer screw. A twin-bladed knife-edged chopper positioned at the entrance to chamber 2 (containing the QMS) allowed the option of chopping the beam at ≃650 Hz.

*Molecular Beam and Mass Spectrometer Detection System.* The molecular beam laser pyrolysis system was constructed from 304 stainless steel with three differentially pumped chambers, each evacuated with oil diffusion pumps with Freon-refrigerated baffles (Figure 2). The second chamber contained an Extranuclear Laboratories quadrupole mass spectrometer with electron impact ionization and ion extraction perpendicular to the beam. The position of the QMS was adjustable from the outside by three screws and a bellows suspension. The bulk of the neutral beam passed through the differentially pumped ionizer region and impinged on a liquid nitrogen cold trap. The cold trap prevented buildup of nitramine in the background gas during operation. The entire pumping system could be degassed by heating up to 200 °C. The ultimate pressure (with no beam) was on the order of $10^{-7}$ Torr in each chamber.

*Data Acquisition.* The mass-selected ions were accelerated into an electron multiplier. With the infrared heating laser off, the CW molecular beam could be chopped, and the signal for a specific ion mass could be phase-sensitively detected by a lock-in amplifier (ITHACO, Dynatrac 391). The QMS could then be accurately tuned into any particular mass by fine adjustment of the mass tuning to give the maximum signal on the lock-in amplifier. The QMS resolution was always better than 0.5 amu and was checked periodically.

With the QMS tuned into a specific mass and with the chopper off, the heating laser was pulsed. The infrared light passed through the cell, and absorption by the $SF_6$, followed by collisional energy transfer to the argon, heated the contents of the cell. Laser light was used to trigger a 1-MHz (sampling rate 1 μs per point) transient digitizer controlled by a DEC LSI 11/23 microprocessor to acquire the QMS signal. To improve signal-to-noise ratios, the signals from 2000 to 3000 laser shots were averaged. As a check that no product buildup was occurring during the experiment, the laser was switched off and the process repeated. In this case, a pulse generator operating at 50 Hz was used to trigger the digitizer. The entire process was repeated for every mass studied. At the end of the experiment, the gain of the ion detector was measured by observing the variation of the CW molecular beam signal with the high voltage. This "gain factor" was found to be mass independent and constant over long periods. The

**TABLE I: Cracking Patterns for DMNA and $NO_2$**

| $m/z$ | cracking (digitizer) | cracking (lock-in amplifier) |
|---|---|---|
| | DMNA | |
| 90 | 1 | 1 |
| 74 | 0.137 | 0.073 |
| 60 | 0.339 | 0.298 |
| 59 | 0.018 | 0.027 |
| 46 | 0.126 | 0.109 |
| 45 | 0.087 | 0.107 |
| 44 | | 0.565 |
| 43 | 2.89 | 2.02 |
| 42 | 3.36 | 2.38 |
| 30 | 0.557 | 0.36 |
| | $NO_2$ (Laser Heated) | |
| 46 | 1 | |
| 30 | 2.1 | |

nitramine reservoir was then removed and the background levels in the vacuum chamber for all masses of interest were measured.

*Data Reduction.* Three operations were carried out on the raw data for each mass to yield the final results. These are briefly described below:

1. The backgrounds were subtracted from the raw data. This operation corrected for all signals not directly from the beam, i.e., background pressure in the ionization chamber.

2. The background-corrected data were then multiplied by an appropriate "gain factor" corresponding to the high voltage used when collecting the signals from that mass. The magnitude of this factor was determined by arbitrarily selecting one voltage as having a gain factor of 1.0 and then calculating the factor for all other voltages. This procedure corrected for the signal enhancement effect of raising the high voltage and allowed direct comparison of the data from different masses.

3. The cracking, or fragmentation, of the dimethylnitramine from the electron impact ionization, rather than thermal decomposition, resulted in substantial increments to some of the lower $m/z$ signals. The magnitude of this contribution was determined in two ways. (a) With the laser off (no thermal decomposition), ac signals (if any) for each mass were read from the lock-in amplifier. These readings were multiplied by the appropriate gain factor (see above), and divided by the reading at $m/z$ 90 for the DMNA molecular ion, to yield the cracking pattern. (b) The digitizer was "pretriggered" to record a signal prior to the laser firing, such that the first millisecond or so of each temporal profile corresponded to unheated gas. Subtraction of the background resulted in a value for the signal analogous to the lock-in reading for each mass. Using this measure of the unheated gas at each ion mass, we also obtained a nitramine cracking pattern.

Both procedures resulted in similar values for the cracking pattern (Table I). The exception was for contributions to $m/z$ 44. No accurate background could be determined for this mass since in order to remove the nitramine reservoir the vacuum had to be broken briefly with subsequent contamination by atmospheric $CO_2$. As a result, only method a could be used for mass 44. Improved cell design is planned to eliminate this problem.

With the contribution to each mass's signal from mass 90 cracking known, it was straightforward to subtract the appropriate fraction of the mass 90 signal from each temporal profile. A similar correction to the $m/z$ 30 ($NO^+$) profile was required to take into account the cracking of $NO_2$. Separate experiments using the present apparatus to produce laser-heated $NO_2$ had given a ($m/z$ 30):($m/z$ 46) ratio of 2.1:1. Thus, once steps 1–3 above had been performed for $m/z$ 46 and 30 ($NO_2$ and NO, respectively), 2.1 times the $m/z$ 46 profile was subtracted from the $m/z$ 30 profile. The extent to which masses other than 90 and 46 fragmented could not be determined quantitatively in the present study. Some contribution at $m/z$ 30 is perhaps expected from the dimethylnitroxyl radical and/or nitrosomethane, but essentially no contribution is expected from dimethylamino radical, dimethylamine, or *N*-methylmethylene imine. In other words, it is highly unlikely that any first- or second-generation (unimo-

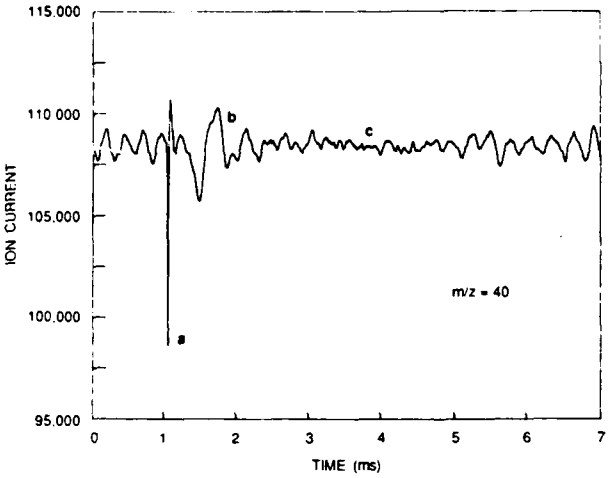


**Figure 3.** Temporal profile for $m/z$ 40: (a) electronic spike, (b) signal fluctuations induced by reflected shock waves, (c) quiescent period.

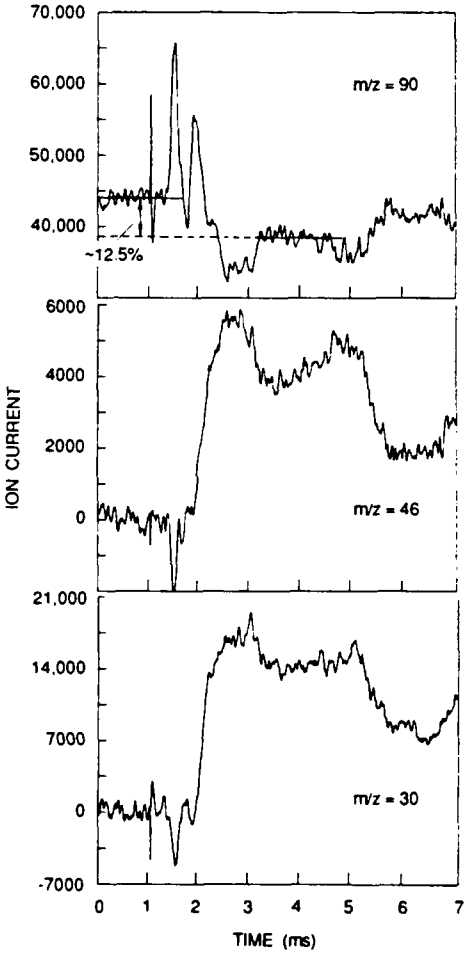


**Figure 4.** Temporal profiles for $m/z$ 90, 46, and 30. Changes in $m/z$ 90 are mirrored by $m/z$ 46 and 30. The rise times for $m/z$ 46 and 30 are identical and correspond exactly to the drop in $m/z$ 90 signal.

lecular) products of $N-NO_2$ bond split, *except* $NO_2$ itself, will make any significant contribution to the $m/z$ 30 signal.

When all of the above corrections had been performed, the resulting temporal profiles corresponded to changes caused solely by the laser-induced thermal decomposition of the dimethylnitramine. Note that we have assumed the cracking pattern for dimethylnitramine is independent of whether the beam is formed from laser-heated nitramine or from near room-temperature nitramine. This is consistent with our molecular beam sampled

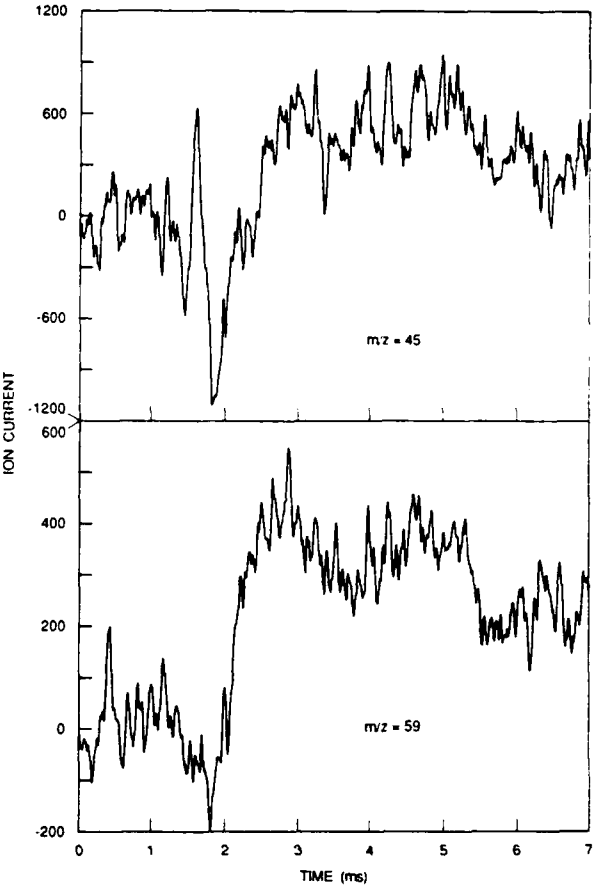


**Figure 5.** Temporal profiles for $m/z$ 45 and 59. Both profiles exhibit the same rise time as $m/z$ 46 and 30.

VLPP work[7,8] with organic substrates, where we find an increase in temperature from 400 to 900 K results in, at most, a small increase in the ratio of a fragment ion signal to that of the parent ion. The heated gas is sampled through a supersonic nozzle expansion which results in rotational and some vibrational cooling. This would tend to reduce any effects of temperature on the cracking pattern. Furthermore, the $m/z$ of most interest here (30, 45, 46, 59, and 60) are not large peaks in the DMNA spectrum, and the corrections to the signal representing NO, $NO_2$, and the dimethylnitroxyl radical are minor. In the particular case of $NO_2$, cracking to give $m/z$ 30, where the correction to the signal that nominally represents NO is large, the cracking pattern was determined for laser-heated $NO_2$. The ratio of $(M = 30)/(M = 46)$ from $NO_2$ increased from 1.93 to 2.10 for laser-heated $NO_2$.

## Results

A typical set of temporal profiles are shown in Figures 3–5. Figure 3 is a temporal profile of the buffer gas, argon. One would expect the signal level before and after the laser pulse to remain unchanged. However, the rapid heating of the reaction mixture propagated a shock wave within the reaction zone. The effects of this shock wave are evident in Figure 3.

It was found necessary to machine an insert for the aluminum block cell to fill as much as possible of the volume unswept by the laser, in order in minimize the effects of the shock waves. These efforts to minimize the cooling and reheating that result from expansion and from reflected shock waves were at least partially successful, and examination of the $m/z$ 40 profile for argon in Figure 3 (and the other figures as well) reveals that they can be divided into several different regions. The first of these

(7) Rossi, M. J.; McMillen, D. F.; Golden, D. M. *J. Phys. Chem.* **1984**, *88*, 5031.

(8) Baldwin, Alan C.; Lewis, K. E.; Golden, D. M. *Int. J. Chem. Kinet.* **1979**, *11*, 529.

regions is from zero time to ~1.2 ms. In Figure 3 this corresponds to unheated argon, as explained above. The sharp spike immediately following this region was caused by the electrical discharge as the laser fired. It acted as a marker for the arrival of the laser light at the reaction cell. The large fluctuations in signal level following the spike were due to shock waves, caused by the rapid heating of the gas, reverberating around the cell and resulting in rapid changes in pressure and temperature. When no $SF_6$ was present, i.e., when no heating occurred, this phenomenon did not occur. The signal returned to a steady level after 2.8 ms. The level during this quiescent period was almost exactly the same as the level prior to the spike. At ~5.0 ms a second series of shock waves were observed. Again, this phenomenon did not occur when there was no heating. All the raw data obtained showed exactly the same shock effects at exactly the same times with the region between 2.8 and 5.0 ms being apparently shock free. From these observations, we concluded that the region from 2.8 to 5.0 ms represented the unperturbed postshock signal level for each mass.

The upper trace in Figure 4 is a temporal profile for dimethylnitramine ($m/z$ 90). The same general features as those for argon can clearly be seen. As explained above, the level prior to the electronic spike corresponds to unheated gas and the level from 2.8 to 5.0 ms corresponds to the level after heating. In this particular case, the nitramine underwent ~12.5% decomposition. Comparison with fractional decompositions observed in laser pyrolysis studies where an internal temperature standard was used[6] indicates that the temperature was about 900 K.

The temporal profile for $m/z$ 46, $NO_2$, is shown in Figure 4. Once again, the same general features can be observed. The reduction in intensity of the spike and the different shock pattern between the spike and 2.8 ms are a direct result of the correction for parent cracking. The subtractions involved in the cracking corrections (see above) do not result in exact cancellation of the spike and shock patterns. To obtain exact cancellation, one would require that the magnitude of the spike and shock patterns for each $m/z$ signal be proportional to the cracking pattern used in the subtraction.

The shock patterns in Figure 4 were typical for all $m/z$ signals, once corrected for cracking. It must be reiterated that the raw data for each mass show the same shock pattern as that for argon and dimethylnitramine. The zero level in Figure 4 for $m/z = 46$, from $t = 0$ to the spike, is genuine; that is, following background, gain, and cracking corrections, this level was indeed zero. This is as it should be, since there was no $NO_2$ present in the original reaction mixture. Had this level not been zero, it would have indicated a buildup of reaction products between laser shots; i.e., the cell contents would not have been fully exchanged between shots. In fact, if the gas flow rate was decreased or the laser repetition rate increased, such a buildup was observed. A second check for product buildup was possible. Signal levels for each $m/z$ were taken with the laser off (no heating) using a pulse generator as digitizer trigger (see above). Signal levels from $t = 0$ to the spike, obtained with the laser firing, were compared with the laser-off values. If buildup were occurring, one would expect these two levels to differ. No such difference was observed. This was found to be the case for all other masses; i.e., the initial zero levels are all genuine.

It is clear from Figure 4 that following the heating there is a sharp increase in the $NO_2$ level. In addition, the rate of increase of the $NO_2$ corresponds exactly with the decrease in the nitramine, indicating that the $NO_2$ was formed at the same time as the nitramine decomposed. This was also found to be the case for the signal change at all $m/z$, with one exception (see below). Figure 4 thus indicates that one thermal decomposition pathway for dimethylnitramine gives nitrogen dioxide as an initial product.

The expected counterpart to $NO_2$ at mass 46 in the DMNA (mass 90) decomposition is the dimethylamino radical (mass 44). There is only a very slight increase in the $m/z$ 44 signal but quite clear increases in the levels of $m/z$ 43 and 42, evidently the principal (and not unexpected) ion fragments of mass 44.

From the direct observation of these initial decomposition products, it is clear that one decomposition pathway involves the cleavage of the N–N bond in dimethylnitramine.

$$(CH_3)_2N\text{–}NO_2 \rightarrow (CH_3)_2N + NO_2 \quad (1)$$

However, these were not the only initial products from the thermal decomposition of dimethylnitramine. Masses 59, 45, and 30 were also produced (Figures 4 and 5). Each of these profiles exhibited the rise time indistinguishable from the rise of $m/z$ 46 and the fall of DMNA at $m/z$ 90. The elapsed time before the periphery of the laser-heated region expands into the nozzle is not more than 10 μs; an upper limit to the fractional reaction of dimethylamino radical and $NO_2$, based on extrapolated literature values[6,9,10] for amino and methyl radical oxidation by $NO_2$, can be placed at ~5%. Thus, in order to explain the production of these species on a time scale appropriate only for a unimolecular reaction, one must invoke a nitro–nitrite rearrangement followed by O–N bond scission in the nitramine, reactions 2 and 3. These

$$(CH_3)_2N\text{–}NO_2 \rightarrow (CH_3)_2NO\text{–}NO \quad (2)$$

$$(CH_3)_2NO\text{–}NO \rightarrow (CH_3)_2NO + NO \quad (3)$$

reactions explain the production of $m/z$ 30 NO. Clearly, one would also expect to see the dimethylnitroxyl radical, $(CH_3)_2NO$ (mass 60). No significant change was observed in the $m/z$ 60 signal. However, the signals at $m/z$ 59 and 45, which would correspond to loss of a hydrogen or a methyl group from the ionzed nitroxyl species, are seen to increase substantially (Figure 5). This fragmentation almost certainly takes place in the ionizer and, given almost no change in the mass 60 signal, is evidently very facile.

From the direct observation of these initial reaction products, it is clear that a second pathway for the thermal decomposition of dimethylnitramine exists involving nitro–nitrite rearrangement followed by O–N bond scission. Calibrations using laser-heated NO and $NO_2$ performed under the same conditions as the dimethylnitramine decomposition indicate that the ratio of rearrangement to simple bond–bond scission ($k_2/k_1$) is about 0.7.

In addition, the apparent mass balance for NO and $NO_2$ production and DMNA loss ranged from 1.05 to 1.33. This was based on the $NO/NO_2$ calibrations and the partial pressure of DMNA measured for the same set of flow conditions. Considering the assumptions made in determining this balance, this is good agreement and suggests that the various spectral subtractions, etc., have not introduced any substantial errors.

Only one other mass showed any discernible change after heating. This was $m/z$ 74, corresponding to the formation of dimethylnitrosamine, $(CH_3)_2N\text{–}NO$. Figure 6 shows temporal profiles for $m/z$ 90, 46, and 74 obtained under conditions where secondary product buildup was occurring. In this case, a very small increase in $m/z$ 74 occurred following the laser heating. However, the rise time was much longer than that for the other masses, supporting the expectation that the formation of dimethylnitrosamine was a result of secondary reactions, presumably the combination of $(CH_3)_2N$ and NO radicals.

## Discussion

The results presented above indicate that, in addition to $N\text{–}NO_2$ bond scission, a substantial fraction of dimethylnitramine (DMNA) decomposes, at temperatures of about 900 K, by way of an intramolecular rearrangement to the N–nitrite, followed by rapid scission of the extremely weak NO–NO bond. The interpretation is straightforward if the results presented above are taken at face value. The certainty attached to these results rests primarily with three factors. The first of these is the extent to which signal changes indicative of chemical reaction can be separated from the effects of reflected shock waves and gas density fluctuations. The second is the extent to which spectral subtraction for $m/z$ 30, 45, 59, and 60 correctly isolates the portions of these signals due to NO and dimethylnitroxyl radical. The third factor is the certainty with which the observed rise time of the $m/z$ 30,

(9) Yamada, F.; Slagle, I. R.; Gutman, D. *Chem. Phys. Lett.* **1981**, *83*, 409.

(10) Slagle, I. R.; Gutman, D. *J. Am. Chem. Soc.* **1982**, *104*, 4741.

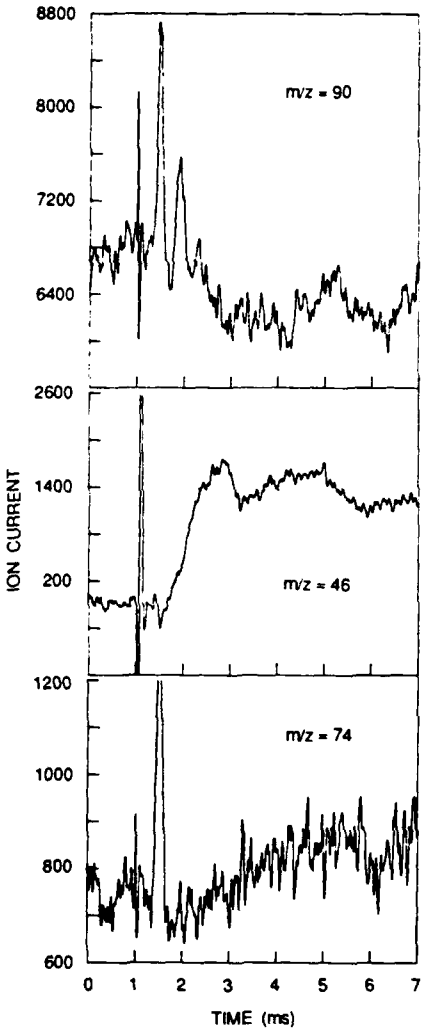


**Figure 6.** Temporal profiles for $m/z$ 90, 46, and 74. Obtained under different conditions than those in Figures 3–5. The rise time for $m/z$ 46 corresponds to the fall in $m/z$ 90. However, the rise time for $m/z$ 74 is much slower than for $m/z$ 46, indicating that this species was formed by secondary reactions.

45, and 59 signals can be stated to be too fast to be accounted for by secondary bimolecular oxidation of dimethylamino radical by $NO_2$. The approach taken to deal appropriately with each of these factors is described in the Results section; these approaches are elaborated below.

In considering the first factor, fluctuations in intensity that are due to reflected shock waves and occur after the arrival of the first laser-heated materials, it should be reiterated that while there are short-term (~250 μs) periodic fluctuations in the $m/z$ 40 signal for the argon carrier due to density changes, there is no change in the signal averaged on a millisecond time scale. Therefore, changes on the latter time scale for reactive components actually reflect chemical changes rather than mere gas density fluctuations. As stated in the Results section, we have chosen as the observation window the interval when the gas density changes reflected in the $m/z$ 40 signal are minimal (3.2–4.5 ms). However, it is important to note that the results are not substantially dependent on this choice of a time window.

Examination of Figure 4, where the $m/z$ 90, 46, and 30 intensities are plotted together, makes it clear that there are three steps of decreasing $m/z$ 46 and 30 intensity (2.3–3.0, 3.6–5.2, and 5.8–6.8 ms) and that these are mirrored by three steps of increasing intensity in the $m/z$ 90 profile. Thus, decreasing amounts of product $NO_2$ correspond to increasing amounts of the starting nitramine. The nozzle is evidently sampling in these three time periods, regions of successively lower values of $\int k\,dt$ or regions

**TABLE II: Change in Ion Current ($t$ = 0–3.5 ms) following Laser Heating**

| $m/z$ | Δ(ion current) | |
|---|---|---|
| 90 | 5500[a] | |
| 60 | ~0 | |
| 59 | 260 | |
| 46[c] | 4260 | $2.9 \times 10^{-9}$ mol cm$^{-3}$ [b] |
| 45 | 660 | |
| 44 | ~0 | |
| 43 | 7421 | |
| 42 | 21310 | |
| 30[d] | 14100 | $2.2 \times 10^{-9}$ mol cm$^{-3}$ [b] |

[a] Corresponds to ~12.5% depletion. [b] Concentrations determined from calibration experiments using $Ar/SF_6/NO_2$ and $Ar/SF_6/NO$ mixtures. [c] Corrected for mass 90 cracking. [d] Corrected for mass 90 and mass 46 cracking.

that have experienced successively greater mixing with the unheated portions of the cell. While we have chosen, for the reason given above, to use the region from ~3.2 to 4.5 ms following the laser pulse, basically the same result is obtained if the region just prior to, or just after, it is used. In these latter regions, there will be somewhat more or somewhat less nitramine decomposition, respectively, and proportionately more or less product appearance from that decomposition. Thus, while the fractional decomposition is dependent on the chosen observation region, the distribution of product masses is not, making it very clear that the changes observed as one samples deeper and deeper into the laser-heated region are *not* the result of (varying extents of) secondary reaction.

The second factor bearing heavily on our principal conclusion is the extent to which ion fragmentation of species other than $NO_2$ and dimethylnitramine (which is quantitatively accounted for in the spectral subtraction) contributes to intensity at $m/z$ 30 and thus might be responsible for apparent rapid production of NO. Dimethylamino radical is not a likely source of $m/z$ 30, since dimethylamine itself has almost no (<2%) intensity at $m/z$ 30. It is, of course, likely that some of the $m/z$ 30 arises from fragmentation of the molecular ion of the dimethylnitroxyl radical, $(CH_3)_2NO$, but this in no way invalidates the main conclusion since the nitroxyl radical is the partner of intramolecularly produced NO. In fact, it is not unexpected that ion fragmentation of nitroxyl radical ($m/z$ 60) might lead via $CH_3NO$ to a substantial fragment at $m/z$ 30. Accordingly, the intensities in Table II reflect use of the mass spectrum of nitrosomethane itself to make a rough estimate of the contribution of the nitroxyl radical to $m/z$ 30. Given that there are no other obvious sources of mass 30, we are left with no alternative but to assign the $m/z$ 30 intensity, once corrected for $NO_2$, $(CH_3)_2NNO_2$, and $CH_3NO$ cracking, to unimolecular production of NO.

Finally, confident assignment of the $m/z$ 30 intensity in Figure 4 to intramolecular production of NO depends on the ability to preclude bimolecular reaction of initially formed dimethylamino radical and $NO_2$ as the source of the nitroxyl radical and NO. As stated in the Results section, the time available for secondary bimolecular reaction is limited to the time before the laser-heated region expands the short distance (<0.1 cm) to the sampling orifice. With this expansion taking place at roughly one-third sonic velocity, the available reaction time is less than 15 μs. With a room-temperature rate constant of $10^{10}$ L/(m$^{-1}$ s$^{-1}$) (with a slight negative temperature dependence, $E$ = –0.6 kcal/mol) as an upper limit for $NO_2$ oxidation of dimethylamino radical (based on measured rates and temperature dependence for $NO_2$ reaction with methyl, amino, and acetyl radicals[6,9-11] and the relevant entropy considerations[12]), one reaches the conclusion that no more than 5% of initially produced $NO_2$ could have been converted to

(11) DeMore, W. B.; Margitan, J. J.; Molina, M. J.; Watson, R. T.; Golden, D. M.; Hampson, R. F.; Kurylo, M. J.; Howard, C. J.; Ravishankara, A. R. "Chemical Kinetics and Photochemical Data for Use in Stratospheric Modeling". National Aeronautics and Space Administration, JPL Publication 85-37.

(12) Benson, S. W. *Thermochemical Kinetics*, 2nd ed.; Wiley: New York, 1976.

NO by bimolecular reaction. Furthermore, as time passes, the expansion proceeds further and the sampling takes place deeper into the laser-heated region. Thus, if secondary reactions were responsible for the observed NO, then the proportion of NO should increase with increasing time. As described in the Results section, such an increase is definitely not observed under the conditions of Figures 3–5. However, if the DMNA reservoir temperature is raised 30 °C and the laser heating is increased so that ~60% of the DMNA is decomposed, then the partial pressures of initially produced $NO_2$ and dimethylamino radicals increase by an order of magnitude each, and the rate of bimolecular production of NO increases by 2 orders of magnitude. Under these conditions, we are able to see the $NO_2$ signal decrease, the NO signal grow substantially during the observation time, and also a growth in $m/z$ 74 (Figure 6) for dimethylnitrosamine.

Because of the desire to have a true real-time measure of the $NO_2$/NO ratios, we are currently exploring the use of laser-induced fluorescence (LIF) to monitor both of these species. This is, in principle, more direct but must deal with possible ambiguities resulting from photochemical generation of NO from $NO_2$, photochemical generation of NO and $NO_2$ from DMNA itself, unknown spectroscopy of radical products, and, at large extents of reaction, with chemiluminescence from secondary reactions.

## Conclusions

The observation of substantial amounts of NO, together with the ion fragments of the dimethylnitroxyl radical, on the same time scale as $NO_2$ is produced, and much too rapidly for significant secondary bimolecular reaction, necessitates the conclusion that this rapidly produced NO arises from an intramolecular nitro–nitrite rearrangement, followed by extremely rapid unimolecular scission of the very weak O–NO bond. Although this is analogous to similar rearrangements that have been reported for nitroalkanes[13] and nitroaromatics,[14,15] it is in contrast with previous reports that dimethylnitramine decomposition proceeds entirely by $N-NO_2$ bond scission.[1-4] At this point, we presume that this reaction proceeds, as those in the $C-NO_2$ cases appear to, as a very "loose" rearrangement with rotation of the $NO_2$ not being substantial until there is considerable lengthening of the $N-NO_2$ bond. The nature of this rearrangement is now being explored in this laboratory (for unsubstituted nitramine) using multiconfiguration ab initio calculations.

*Acknowledgment.* We acknowledge the support of the U.S. Army Research Office under Contract No. DAACO3-86-K-003 and the U.S. Air Force Office of Scientific Research under Contract No. F496220-85-K-00006. The Chemical Physics Laboratory computer system (VAX 11/750) was purchased under NSF Grant PHY-8114611.

**Registry No.** DMNA, 4164-28-7.

(13) Wodtke, A. M.; Hintsa, E. J.; Lee, Y. T. *J. Phys. Chem.* **1986**, *90*, 3549.
(14) Gonzalez, A. C.; Larson, C. W.; McMillen, D. F.; Golden, D. M. *J. Phys. Chem.* **1985**, *89*, 4809.
(15) Tsang, W.; Robaugh, D.; Mallar, W. G. *J. Phys. Chem.* **1986**, *90*, 5968.

# Appendix C

## SYNTHESIS OF N,N-DIMETHYLNITRAMINE BY NITRODEPHOSPHORYLATION OF HEXAMETHYLPHOSPHORAMIDE

Reprinted from The Journal of Organic Chemistry, 1988, Vol. 53, page 4140


# Synthesis of *N,N*-Dimethylnitramine by Nitrodephosphorylation of Hexamethylphosphoramide

Jeffrey C. Bottaro,* Clifford D. Bedford, Robert J. Schmitt, and Donald F. McMillen

*Energetic Materials Program, SRI International, 333 Ravenswood Avenue, Menlo Park, California 94025*

*Received March 3, 1988*

The large-scale synthesis of *N,N*-dimethylnitramine[1,2] poses serious safety problems resulting primarily from the formation of nitrosamine byproduct and the use of potentially explosive mixtures of nitric acid and acetic or trifluoroacetic anhydride.[3,4] In addition, the use of the highly oxidizable amide, dimethylformamide, increases the changes of thermal runaway during the nitration process. In our search for a safe, pilot-plant-scale synthesis of this material (not currently available commercially), we examined the ostensibly exothermic metathesis of a phosphoryl amine with nitric acid—in this case hexamethylphosphoramide (HMPA)—to give dimethylnitramine and phosphoric acid (eq 1). This approach utilizes amides of

$$[(CH_3)_2N]_3P{=}O + 3HONO_2 \rightarrow (HO_3)P{=}O + 3(CH_3)_2NNO_2 \quad (1)$$

phosphoric acid, rather than formic acid, thus circumventing some of the potential oxidative side reactions of *N,N*-dimethylformamide and similar carboxylic acid amides under typical nitration conditions.

This synthesis has proved viable in practice. We isolated a 200% yield of *N,N*-dimethylnitramine and only a small amount (12%) of the carcinogenic *N,N*-dimethylnitrosamine impurity when the reaction was run on roughly a half-mole scale, based on starting HMPA. The reaction was run between 0 and 10 °C; ice-bath cooling was required. The products were isolated by neutralization with

(1) Robson, J. H.; Reinhart, J. *J. Am. Chem. Soc.* **1955**, *77*, 2453.
(2) Robson, J. H.; Reinhart, J. *J. Am. Chem. Soc.* **1955**, *77*, 107.
(3) Bedford, C. D. *Chem. Eng. News* **1980**, *58*(35), 33 and 43.
(4) Coon, C. Lawrence Livermore National Laboratory, 1987 (personal communication).

cooling, followed by chloroform extraction.

Notably, only two of the three dimethylamino ligands underwent nitration to give a 200% yield, rather than all three giving the maximum possible 300% yield of the desired product. Further study will reveal the fate of the currently unaccounted for dimethylamino ligand.

The implications of this observation for explosive technology are significant. A phosphorus-based scaffold might be feasible as an incipient polynitramine framework, with use of variations on the reaction described here. Elaborations of this methodology are being investigated.

## Experimental Section

*Caution! This procedure produces traces of N,N-dimethylnitrosamine, a known carcinogen.*

Hexamethylphosphoramide (50 g, 0.28 mol) was added dropwise to a stirred mass of 600 g (400 mL) of 100% nitric acid in a 1-L flask cooled by an ice bath. The rate of addition was carefully regulated to prevent the reaction mixture from ever heating beyond 10 °C; the addition time was approximately 90 min. After the addition was complete, the reaction mixture was allowed to warm to room temperature over an additional 90 min. Workup was carried out by quenching the reaction mixture into 1 kg of ice, neutralizing with 400 g of NaOH with ice cooling of the diluted mixture, and extracting with 3 × 200 mL of chloroform. Drying, filtering, and concentrating, followed by crystallization from carbon tetrachloride, gave 50 g (200%) of *N,N*-dimethylnitramine, mp 53–55 °C. The mother liquor yielded 3 g (12%) of dimethylnitrosamine, a yellow liquid with nonequivalent methyls in its NMR spectrum. *N,N*-Dimethylnitramine does not pose a significant explosion hazard under normal laboratory conditions. It should be kept from exposure to extreme heat (>150 °C).

**Acknowledgment.** We wish to thank the Army Research Office (Contract No. DAAC03-86-K-0030) and the Air Force Office of Scientific Research (Contract No. F49620-85-K-00006) for support of this research.

**Registry No.** $[(CH_3)_2N]_3P{=}O$, 680-31-9; $HONO_2$, 7697-37-2; $(CH_3)_2NNO_2$, 4164-28-7.

# Appendix D

## LASER-INDUCED FLUORESCENCE DETECTION OF $NO_2$ AND NO FROM THE THERMAL DECOMPOSITION OF DIMETHYLNITRAMINE

# LASER-INDUCED FLUORESCENCE DETECTION OF $NO_2$ AND NO FROM THE THERMAL DECOMPOSITION OF DIMETHYLNITRAMINE

## INTRODUCTION

In this Appendix,we describe efforts using laser-induced fluorescence (LIF) measurements of NO and $NO_2$ concentrations on the microsecond time scale, thereby precluding interference from rapid bimolecular secondary reactions. With these measurements, we had hoped to determine the branching between initial N-$NO_2$ bond scission and nitro-nitrite rearrangement in the decomposition of dimethylnitramine (DMNA). This effort represents (1) an approach that was not spelled out in the original proposal, but was clearly called for by the results of the work in progress, and (2) work that was not completed by the time the project ended, but was interesting in itself, and that establishes the conditions for making the desired branching ratio measurements under conditions that will provide unequivocal results.

As discussed in Appendices A and B,[1,2] cleavage of the N-$NO_2$ bond to produce $NO_2$ and the dimethylamino radical (reaction 1) was originally expected to be the dominant unimolecular decomposition pathway in the high-temperature thermal decomposition of dimethylnitramine . The basis for this expectation was, first, the fact that the N-$NO_2$ bond is the weakest bond in DMNA,[3] and, second, most previous DMNA studies[4-6] have invoked it as the rate-determining step under a variety of conditions. In some of these studies,[4] however, the ultimate product mixture cannot be quantitatively accounted for by a

sequence of known or plausible reactions following an initial N-$NO_2$ scission. In others,[6] autocatalytic behavior is observed that is not fully consistent with rate-limiting thermolysis. Schroeder[7] and Melius et al.[8] have discussed the possibility of H-atom (or other radical) attack on nitramines as the first step in the oxidation of radicals by closed-shell nitramines. Furthermore, previous studies in this laboratory[1,2,9] have found evidence for other pathways, bimolecular as well as unimolecular, that tend to be more competitive than analogous reactions in simple hydrocarbons.

At low temperatures, where concerted, low activation energy processes will be relatively favored, HONO elimination is expected as a possibility, by analogy with aliphatic C-$NO_2$ compounds. This reaction has in fact been reported in low-temperature, low-pressure Knudsen cell studies,[9] where the high A-factor thermolysis process has been additionally suppressed by being in the unimolecular fall-off region. However, in the more recent work described in the preceding Appendices[1,2] the evidence indicates that still another unimolecular decomposition pathway is operative in the 800°C vicinity. This reaction involves rearrangement to a weakly bonded nitrite intermediate that undergoes very rapid thermolysis to the dimethylnitroxyl radical and NO, (reactions 2 and 3).

| | | | | |
|---|---|---|---|---|
| (1) | $Me_2N\text{-}NO_2$ | → | $Me_2N\cdot + NO_2$ | $k_1$ |
| (2) | $Me_2N\text{-}NO_2$ | → | $Me_2NONO$ | $k_2$ |
| (3) | $Me_2NONO$ | → | $Me_2NO\cdot + NO$ | $k_3$ |
| (4) | $Me_2N\cdot + NO_2$ | → | $Me_2NONO$ | $k_4$ |

Reaction (2) had not been previously reported for any nitramine,[4-6] but the analogous rearrangement has been observed for nitromethane[10] and nitrobenzene.[11,12] Based on the kinetic model for the decomposition of dimethylnitramine developed by Nigenda et al.,[1] the initial rearrangement of the starting material to form the nitrite is one of the rate-determining steps in NO production. The fitted rate constants obtained by Nigenda for reactions (1) and (2) are roughly equal at 900 K, with $NO_2$ formation favored at higher temperatures and

nitrite formation favored at lower temperatures (Table 1). Since nitro-nitrite rearrangement (Reaction 2) leads to the same products as thermolysis followed by recombination on oxygen (Reactions 1 and 4), this fitting was dictated largely by the observed overall temperature-dependence of DMNA decomposition. Therefore, because of the ever-present danger that measured activation energies for the nominal rate-determining step in a complex reaction system will be distorted by systematic error, the results of Nigenda,[1] however compelling, could not be considered fully definitive. Accordingly, Stewart et al. studied DMNA decomposition using a laser-pyrolysis apparatus in which the laser-heated region expands into the orifice of a molecular-beam sampling system.[2]

Table 1

Rate constants at several temperatures for reaction s (1) through (4).
Arrhenius parameters taken from Nigenda et al.[1]

| Reaction | Log A | $E_a$ (kcal/mole) | $t_{1/2}$ 700 K | $t_{1/2}$ 900 K | $t_{1/2}$ 1000 K |
|---|---|---|---|---|---|
| (1) | 15.3 | 46.5 | 100 ms | 68 μs | 5.0 μs |
| (2) | 11.5 | 31.0 | 10 ms | 74 μs | 13 μs |
| (3) | 13.7 | 9.0 | 9 ps | 2.1 ps | 1.3 ps |
| (4) | 10.0 | 0.0 | 50 μs[a] | 70 μs[a] | 80 μs[a] |

[a]Estimated lifetime for the bimolecular recombination (or oxidation) reaction at the indicated temperature and under conditions of the molecular-beam studies of Reference 2 (i.e., 10% decomposition of 500 mtorr DMNA).

In the work of Stewart, both $NO_2$ and NO were observed to appear simultaneously and in relative amounts that were not dependent on the initial DMNA partial pressure or on the fractional decomposition.[2] Thus, the appearance of NO was not consistent with its formation in a secondary bimolecular reaction. Nevertheless, the times required for the leading and trailing portions of the laser-heated region to expand into the sampling orifice were roughly 10 and 100 μs, respectively The estimated half-lives shown in Table 1 show

that facile secondary reactions (such as radical recombinations, whose low temperature dependence means they will not be substantially slowed by the ~200 K adiabatic expansion cooling that occurs after about 10 μs) could not be *a-priori* ruled out on the millisecond time scale.

Finally, large basis set *ab-initio* quantum mechanical calculations (for $NH_2NO_2$ ) by Saxon and Yoshimine[13] indicate that there is a barrier on the route to the nitrite that is of similar energy to that required for simple N-$NO_2$ bond scission. Unfortunately, while this latter result is in qualitative agreement with the GC-MS-monitored results of Nigenda et al., it does not suggest an A-factor for the rearrangement as low as that extracted through their kinetic fitting.

To summarize the preexisting situation with dimethylnitramine, much evidence has been obtained for a competitor to simple N-$NO_2$ scission as the initial decomposition step. However, no completely definitive or quantitatively consistent picture has emerged to unequivocally displace the reports in the literature that have interpreted DMNA decomposition simply in terms of initial N-$NO_2$ bond thermolysis.[4-6] Therefore, determination of the products formed from DMNA decomposition on the submillisecond time scale where rapid bimolecular reactions are wholly precluded, is desirable in order to make a definitive statement about the branching between thermolysis and nitro-nitrite rearrangement. Such a statement, in turn, is necessary if there is ever to be a mechanistically useful understanding of the functioning of nitramine-based energetic materials.

Because laser-induced fluorescence is a highly sensitive, nonintrusive technique capable of determining concentrations on a microsecond time scale and has previously been used[14-16] for measurement of both NO and $NO_2$, we decided to use this approach to measure these species immediately following the IR laser pulse. The product temporal concentration profiles should yield additional information on the initial unimolecular decomposition process and should either provide conclusive evidence of NO production as

a result of unimolecular decomposition through a rearrangement (reactions 1 and 3) or show that, after all, the sole source of NO is the rapid secondary bimolecular reaction between $NO_2$ and the dimethylamino radical (reaction 4). On the microsecond time scale of the LIF measurements and a total pressure of 40 Torr, bimolecular reactions will not have occurred. As shown in Table 1, the parameters obtained in our previous studies[1] lead one to expect an equal yield of NO and $NO_2$ from the unimolecular decomposition of DMNA at about 900 K.

## EXPERIMENTAL PROCEDURE

### REACTION CELL

A chamber (1.2 liter) with three sets of mutually perpendicular optical windows was used to study the laser pyrolysis of DMNA (Figure 1). Infrared laser light from either a Tachisto or Lumonics $CO_2$ laser [1P(20) line at 10.6 mm] was passed through 6-mm-thick KCl windows and reflected back through the cell (2.5-cm path length). The dye laser was aligned orthogonal to the $CO_2$ laser so as to sample a small volume of the irradiated region in the reaction vessel. In the third direction, fluorescence light was collected. A slow flow consisting of DMNA, $SF_6$, and Ar was maintained through the cell. This gas flow was provided by passing an $SF_6$-Ar mixture through a tube of solid DMNA to obtain a DMNA partial pressure of about 0.5 mtorr. The $CO_2$ laser pulse heats the mixture to the reaction temperature in 2-3 mm, and reaction takes place at the peak temperature until the axially symmetric expansion wave, traveling radially inward from the periphery of the cylindrical laser-heated region, reaches the center.

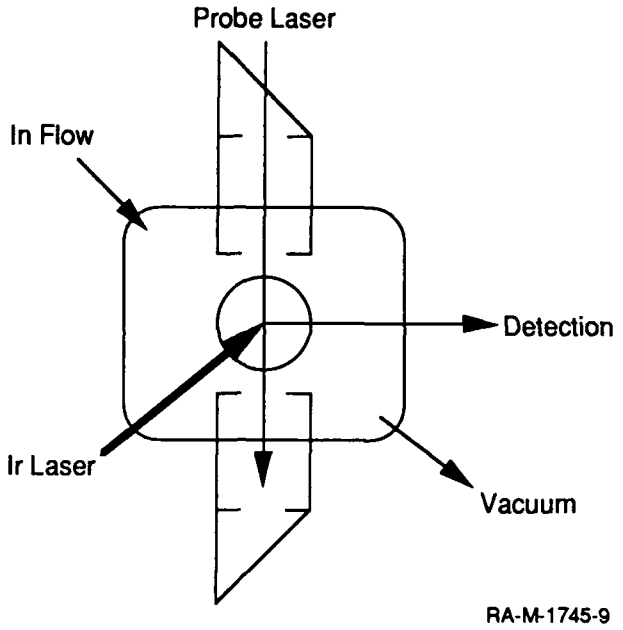


Figure 1. Schematic of reaction cell.

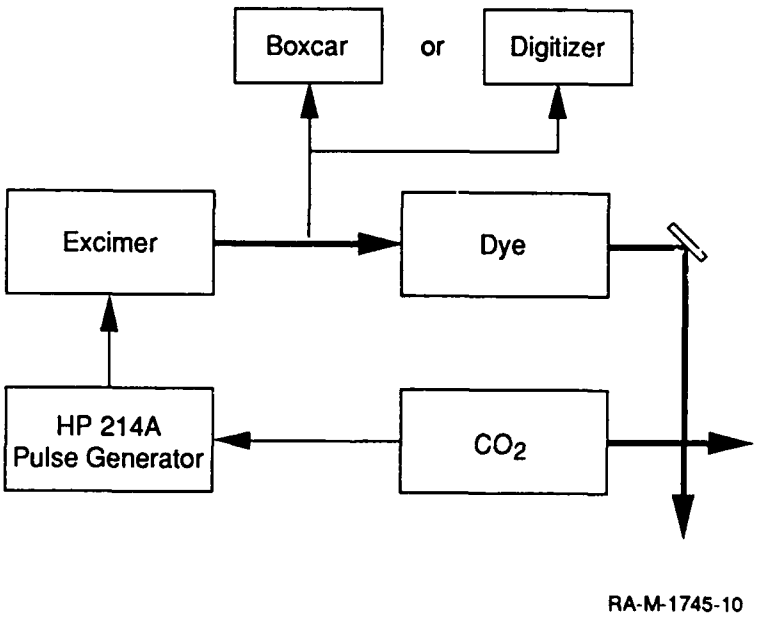


Figure 2. Schematic of timing sequence of lasers and detection.

The repetition rate of the $CO_2$ laser was held to a value (0.5-2 Hz) such that the 2.5-$cm^3$ irradiated volume was largely cleared (by diffusional mixing), of products from one pulse before the next pulse again heated the reaction mixture. Since the characteristic diffusion time for a distance of 5 cm is about 5 s at our operating pressures (40 torr), complete mixing in our cell requires 10-25 s. However, the heated volume of 2.5 $cm^3$ would diffusionally mix with the surrounding 50 $cm^3$ in only about 1 second, lowering the product concentrations to ~5% of their maximum values. In addition, it is anticipated that the mixing will be convectively aided to a considerable degree. All results obtained at 0.5-2 Hz were found to be consistent with these expectations.

The timing delay between the $CO_2$ laser and the probe laser was obtained with a HP 214A pulse generator triggered with a synchronized signal from the firing of the $CO_2$ laser (Figure 2). Stray light from the excimer laser was collected with a photodiode and used to trigger the boxcar or digitizer detection electronics.

## LASER-INDUCED FLUORESCENCE DETECTION

LIF is commonly used for detecting NO and $NO_2$ on an individual basis.[14,15] However, LIF detection of NO in the presence of substantial amounts of $NO_2$ is subject to complications, as will be discussed. Our approach to measuring NO in the presence of $NO_2$ is based on the method of Alder et al.,[16] in which two-photon exitation of NO was accomplished with focused light of 452 nm. Single-photon excitation of $NO_2$ was accomplished, as is common practice,[15] with unfocused 452-nm radiation.

$$h\nu\ (452\ nm) + NO_2 \rightarrow NO_2^* \rightarrow NO_2 + h\nu\ (visible)$$
$$2h\nu\ (452\ nm) + NO \rightarrow NO^* \rightarrow NO + h\nu\ (UV)$$

### $NO_2$ Measurement.

Light at 452 nm (pulse width of 37 ns) was obtained from a Lambda Physik FL2002 dye laser (coumarin-450) pumped with a Lumonics Hyperex-400 XeCl excimer laser. Since single-photon excitation of the $NO_2$ with 452-nm light results in broad-band visible fluorescence, a three-lens borosilicate optical system (Figure 3) was used in imaging a small volume of this fluorescence through two yellow cut-off filters (Corning 3-69 and 3-70; $l > 520$ nm) onto a RCA 1P28A photomultiplier tube. The first glass abstraction lens was 3 cm in diameter with a focal length of 2.65 cm. The signal was amplified and measured with a SRS boxcar or digitally stored on a computer. The long-lived fluorescence of $NO_2$ is rapidly quenched by most gas molecules (including all those used in this study). This provides a narrow fluorescence signal that must be observed well up on the tail of the excitation pulse and thus requires filtering the scattered laser light.

### NO Measurement.

Excitation of NO was obtained in a two-photon process by focusing the 452-nm light (40-cm focusing lens). This selectively populates the $A^2S^+$ state through the 0,0 transition. The g band UV fluorescence of NO ($A^2S^+ \rightarrow X^2P$) was observed with a single lens (quartz, 4-cm diameter, 5-cm focal length) setup (Figure 4) through a 3-mm Schott UG-11 filter (280-380 nm) by the same detection electronics described above. This collects emission from the 0,5 and above fluorescence transitions.

In part of this study we investigated the fluorescence spectrum with a 218 McPherson 0.3-meter scanning monochromator and an OMA I diode array detector. Calibration of this detection system was done with a Hg lamp. The three-lens optical detection system was used, which limited the lower detection wavelength to 330 nm since glass lenses were used.

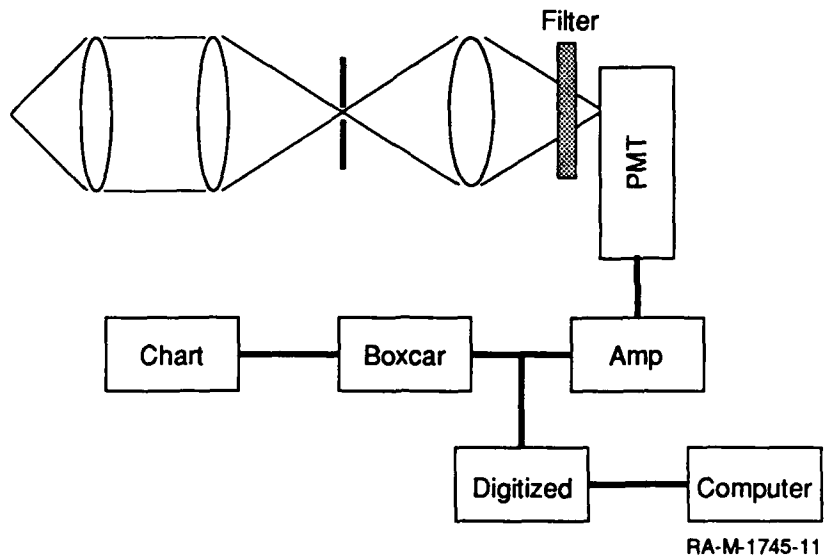


Figure 3. Optical detection scheme for $NO_2$ and detection electronics.

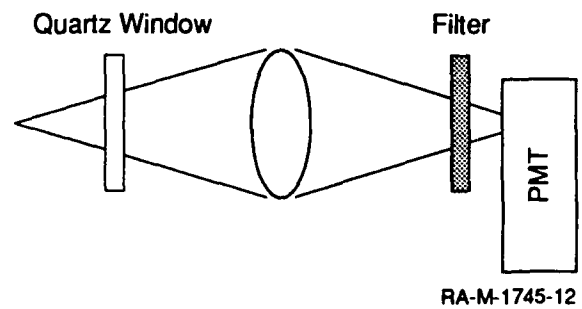


Figure 4. Optical detection scheme for NO fluorescence.

## TEMPERATURE DETERMINATION

To compare the absolute values of the rate constants determined here with kinetic models derived from previous studies,[1] we must know the reaction temperature at the location where the concentrations were measured. Determining the reaction temperature using the LIF excitation spectrum of a small diatomic molecule was convenient. We used the rotational temperature of NO as the thermometer. Ozaki et al. showed that this was an accurate method in the 300-470 K temperature range.[17] McKenzie et al. used this method to determine the temperature in unsteady gas dynamic processes below 300 K.[18] Figure 5 shows a typical Boltzman plot obtained from the two-photon excitation spectrum on NO using the rotational levels 6.5-23.5 of the $\gamma$ band $R_{11}+Q_{21}$ branch. This spectrum corresponds to a temperature of approximately 700K.

# RESULTS

Measured signal intensities for both NO and $NO_2$ are time- and concentration-dependent (Figure 6). At a given concentration, the measured signal increases with time after infrared irradiation up to about 20 $\mu$s, when the expansion-wave cooling reaches the center of the cell, and then begins to decrease slowly (Figure 7). This decrease is likely due both to a decrease in density caused by expansion at times greater than 20 $\mu$s The decrease in signal intensity with time is also dependent on the concentration. In Figure 6(b), plots at two delay times following IR irradiation (1.8 and 15 $\mu$s) show the slope of signal intensity versus NO concentration to decrease as the time between the heating pulse and the probe laser pulse increases. This behavior was also observed for $NO_2$, as shown in Figure 6(c).

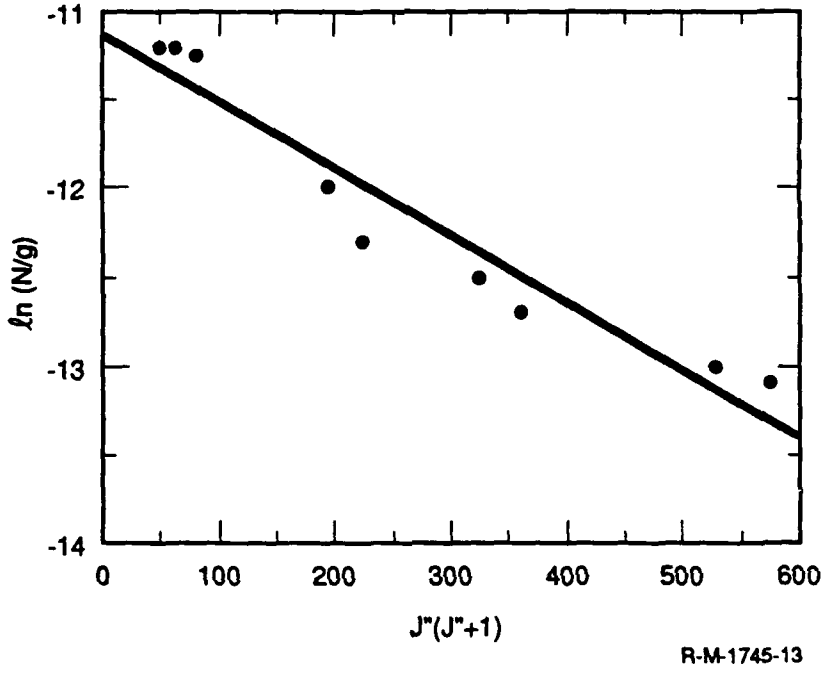


Figure 5. Boltzman plot of NO rotational levels 6.5-23.5 of the γ band $R_{11} + Q_{21}$ branch from the two-photon excitation spectrum obtained 2 μs after irradiation with the infrared laser.

Infrared laser power 0.9 J/pulse, 40 torr 10% $SF_6$/Ar.

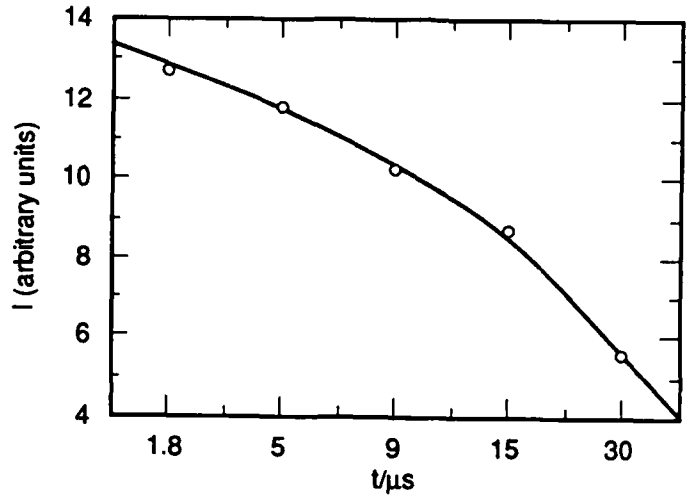


(a) Signal intensity versus time for 30 mtorr NO.

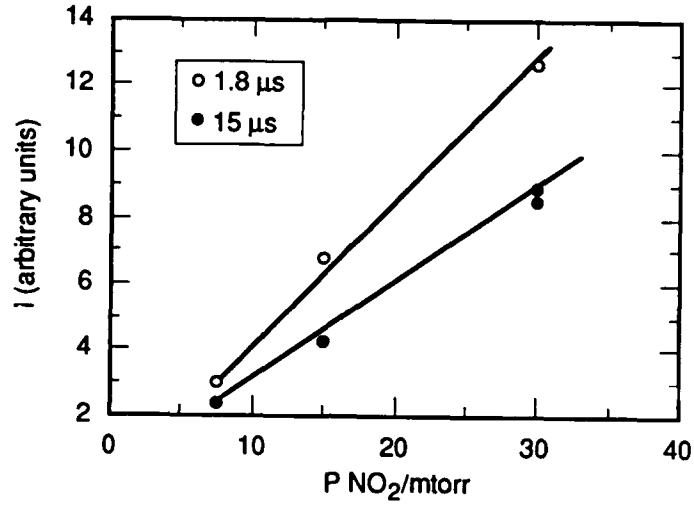


(b) Signal intensity versus NO partial pressure at 1.8 and 15 μs after IR irradiation.

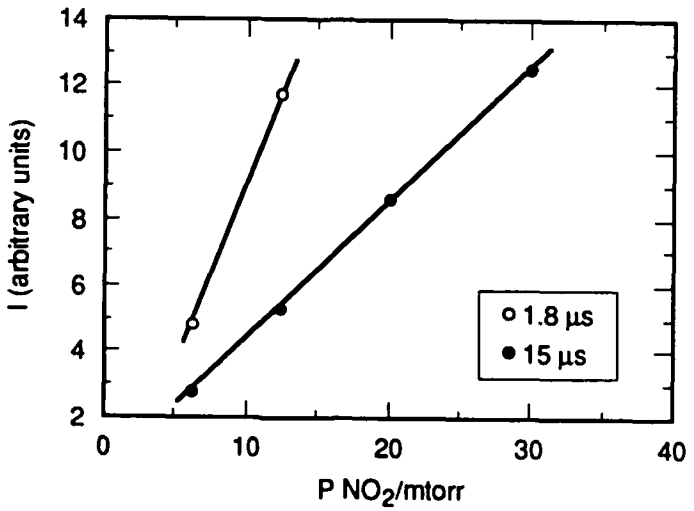


(c) Signal intensity versus $NO_2$ partial pressure at 1.8 and 15 μs after IR irradiation.

RA-1745-14

Figure 6. Measured fluorescence intensity dependence on NO and $NO_2$ concentrations in 40 torr 10% $SF_6$ /Ar.

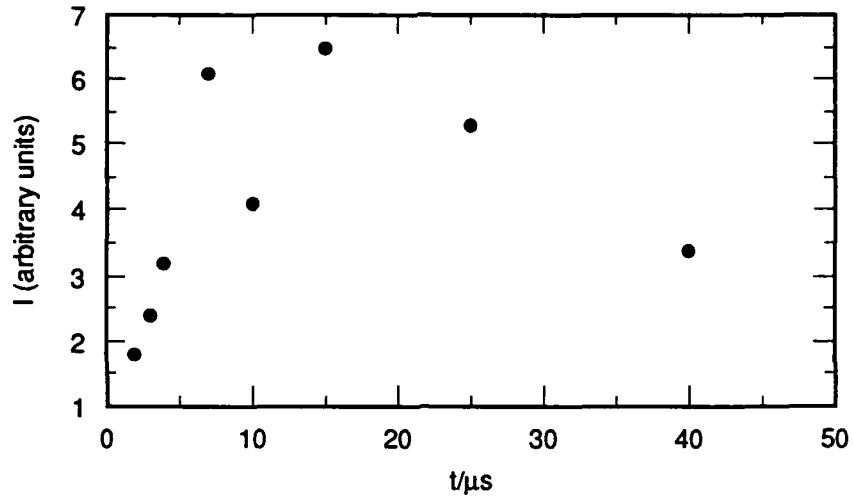


(a) 1.05 J/pulse

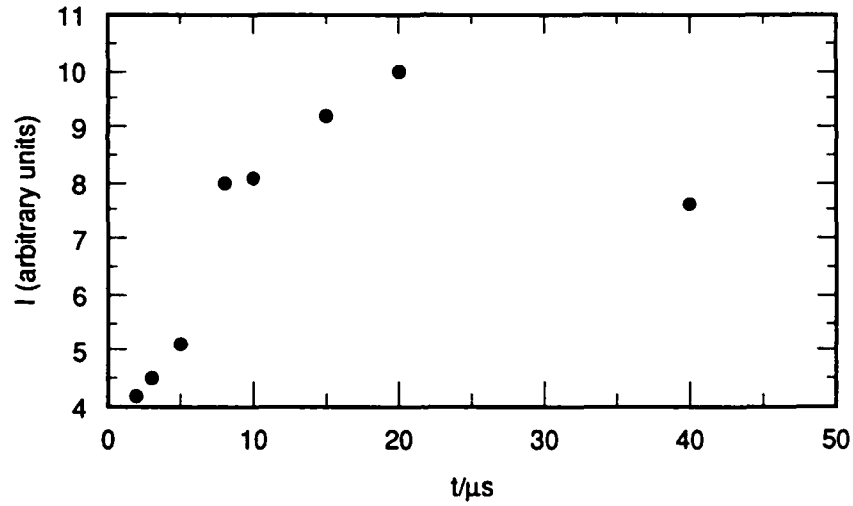


(b) 1.15 J/pulse

RA-M-1745-15

Figure 7. $NO_2$ concentration as a function of time.

Several complications in the task of quantitatively relating fluorescence intensity to concentration can be envisioned and have been experimentally addressed. First, a 1+1 photo addition to $NO_2$ with 452 nm light would provide enough energy for decomposition, providing a spurious source of NO. Such decomposition would occur only while focusing the probe laser during NO detection. The probable products NO + O would interfere with the detection of NO. We observe a spurious NO signal from $NO_2$. This complication is amenable to use of an NO correction factor that is based on the concentration of $NO_2$.

A second possible complication is the photodissociation of dimethylnitramine (DMNA) initiated by the 452-nm light. In the solution phase, UV-Vis absorption of DMNA starts at 300 nm (solvents: $CH_2Cl_2$ and MeOH), so the decomposition of DMNA by single-photon addition should not be a problem (assuming similar absorption characteristics at 900 K in the gas-phase as is found in solution at 305K). However, multiphoton excitation may lead to decomposition. This possibility was experimentally addressed by LIF analysis before and after the initiation of pyrolysis. This procedure produced no evidence for the photochemical dissociation of DMNA by the focused probe laser at 452 nm.

A third possible complication has thus far provided the greatest obstacle to obtaining the desired measurements. Following pyrolysis of DMNA (P = 32 torr 10% $SF_6$/Ar), we observed luminescence in the UV and visible without the probe laser (Figure 8). We assigned this emission to CN ($B^2S \rightarrow X^2S^+$, 385 nm), CC ($A^3P_g \rightarrow X^3P_u$, 515 nm), and CH ($A^2D \rightarrow X^2P$, 432 nm) species. The UV emission from CN overlaps the induced fluorescence from NO, leading to an artificial signal. At high enough incident IR laser fluences (>1.2 J/cm$^2$), this emission was apparent to the naked eye as a purple glow (CH fluorescence).

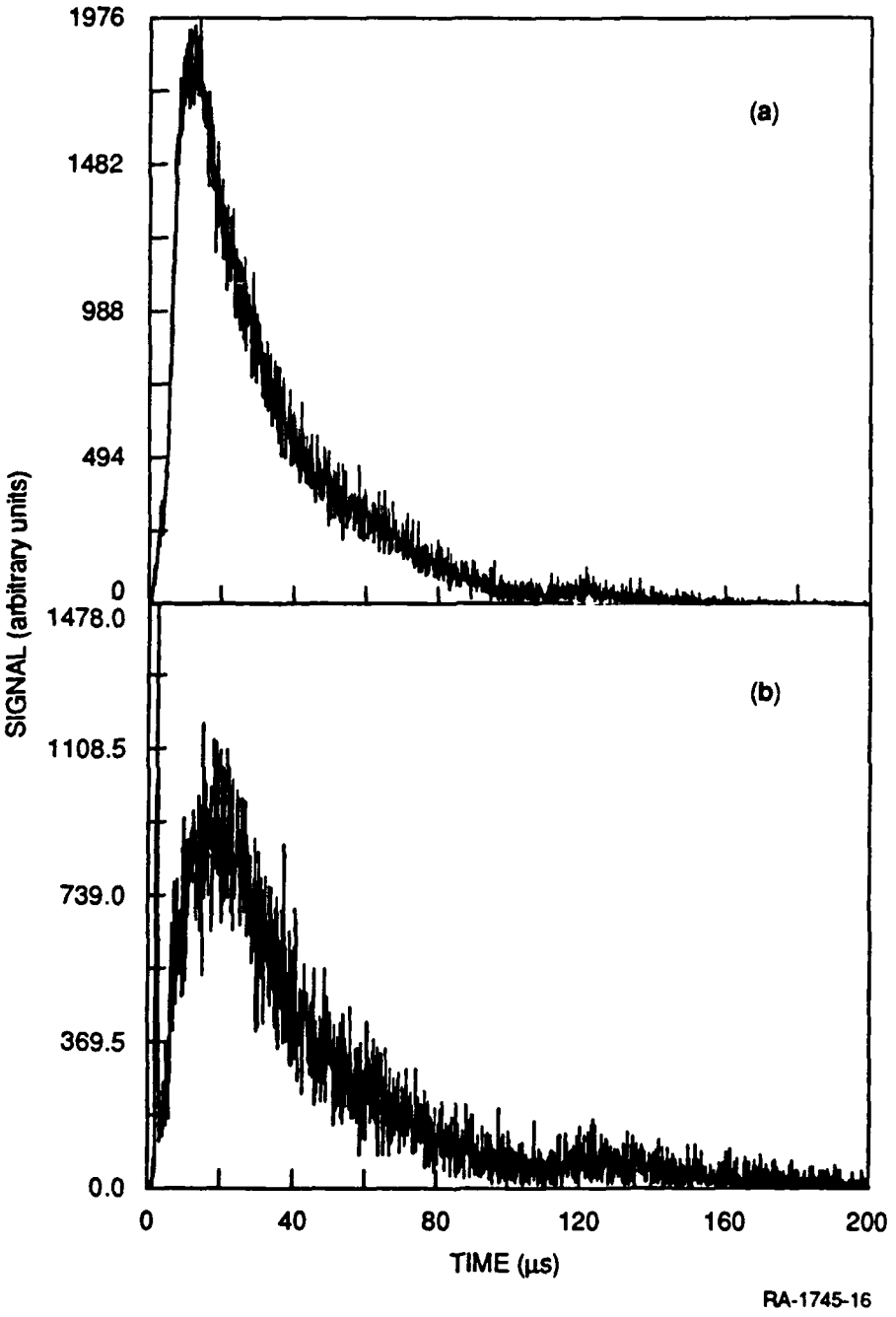


Figure 8. Chemiluminescence signal observed up to 200 μs after IR irradiation (1.5 J/pulse) of DMNA.

(a) Luminescence observed from 280-380 nm. (b) Luminescence observed from 360-700 nm.

To further investigate this spontaneous emission, we examined the pyrolysis of nitromethane, dimethylamine, isobutene, and isobutane (400-mtorr substrate in 32 torr 10% $SF_6$/Ar); the relative intensities are shown in Figure 9. No emission was observed in the pyrolysis of the hydrocarbons until fluences greater than 1.8 J/cm$^2$. This fluorescence consisted primarily of CH emission, being somewhat greater for the saturated hydrocarbon than for the olefin. In contrast, at fluences as low as 0.8 J/cm$^2$, fluorescence from CN, CC, and CH was observed in the pyrolysis of dimethylamine, similar to that observed with DMNA. With nitromethane, CN emission was observed at fluences of 0.7 J/cm$^2$. Emission from CN in the pyrolysis of DMNA was greater than that observed from dimethylamine and nitromethane.

The luminescence from DMNA was investigated as a function of bath gas (Ar, $CO_2$, and $CF_4$). At 3 torr $SF_6$ and 30 torr bath gas pressure (0.75 J/cm$^2$), UV emission was observed only with Ar. With $CO_2$ and $CF_4$ bath gases, luminescence was not observed unless the pressure of $SF_6$ was 8 torr or higher. For a given $SF_6$ pressure, not only the temperatures, but also the infrared absorption, are higher when argon is the bath gas. For a given amount of absorbed radiation, the lower heat capacity of argon would, of course, lead to a higher temperature. In addition, the red shift of the $SF_6$ absorption at higher temperatures coincides better with the P-20 line of the IR laser. Thus, with Ar, the temperature is higher both because more IR is absorbed and because a given radiative input results in a larger temperature increase.

Measurement of $NO_2$ concentration at two low $CO_2$ laser fluences (0.26 and 0.33 J/cm$^2$) provided us with two concentrations (40 and 60 mtorr, respectively). These correspond to temperatures based on the previously determined parameters for decomposition of 890K and 910K, respectively. These temperatures are somewhat higher than those estimated from the absorbed energy and heat capacities (580 and 650 K, respectively in the two cases).

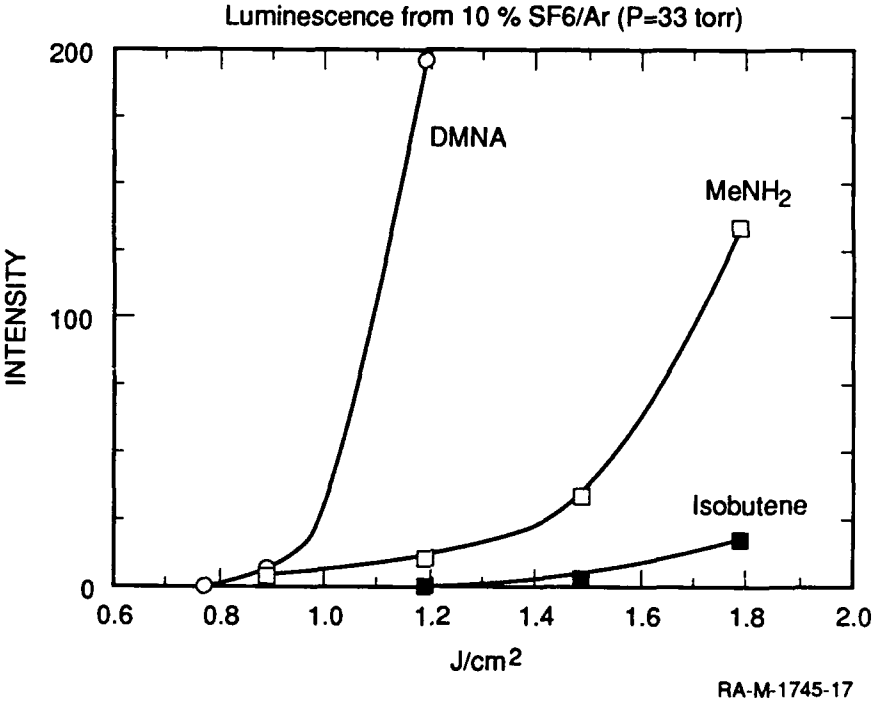


Figure 9. Luminescence from heating various substrates as a function of $CO_2$ laser fluence.

For DMNA and $Me_2NH$, CN emission was monitored; CH emission was monitored for isobutene.

## DISCUSSION

The emission from CN, which has thus far prevented a definitive measure of NO and $NO_2$, has been observed in many systems with and without a nominal source of carbon. For example, in the decomposition of $FN_3$, only CN fluorescence was observed, presumably from wall interactions. Fluorescence from CN is also prominent from bow shock in the atmosphere. Since CN is a good emitter, the light we saw may have been due to a very small concentration of CN and therefore does not necessarily represent interference with the unimolecular kinetics we wish to observe. The remaining question, though, is how CN originates from DMNA in such a short time when several reaction steps must be required. Some of these reactions would have to be either bimolecular or, if they were unimolecular, the result of very high temperatures. Such high temperatures could conceivably result from hot spots in the $CO_2$ laser. Although we expect that hot spots are not likely to be so intense that they provide temperatures sufficient that the entire sequence of three unimolecular reactions required to generate CN from dimethylnitramine would occur in 4 μs, substantial effort was made to eliminate any possible hot spots. This effort did not result in the significant decrease in the chemiluminescence resulting from laser-heating of the dimethylnitramine.

The possibilities of infrared multiphoton decomposition or decomposition under energy-transfer-limited conditions need to be considered in the present case. In the case of the second possibility, results published by Mele et al.[19] indicate that $SF_6$-sensitized decompositions at pressures of 10 to 30 Torr proceed under nonequilibrium conditions. However, because these workers used a focused IR laser beam of only 0.1 cm diameter, their reaction times before expansion cooling would be extremely short (< 0.5 μs). Furthermore, reaction under energy-transfer-limited conditions would be less, rather than

more, likely to result in the energization necessary to give rise to a sequence of unimolcular reactions that could give rise to CN in 4 μs.

In the case of possible multiphoton decomposition, high-"temperature" reaction is of course a possibility (DMNA has an absorption at about 10 μm), but very high fluences are typically required to pump by the lowest energy reaction channels. In our original GC-MS-monitored laser pyrolysis studies,[1] the laser-heated reaction mixtures were generally at 100 torr total pressure, the bath gas was $CO_2$, rather than Ar, and there was no evidence of multiphoton reaction. It seems highly unlikely that a two-fold decrease in total pressure, even with a less effective collider molecule, could result in the degree of multiphoton heating necessary to produce CN in 4 μs.

In summary, the question of how the CN emission arises so quickly is very interesting and worth investigating in itself. Short of that, it may be possible to eliminate the chemiluminescene by performing the LIF measurements using $CO_2$ as a bath gas. However, $CO_2$ is much more effective at quenching the LIF signal, and it may be difficult to obtain the required signal intensity when it is the major bath gas. An additional possibility for direct determination of NO and $NO_2$ on the microsecond time scale is resonant multiphoton ionization (REMPI). This technique has been used previously for NO measurement in combustion environments.[20] The capability to perform such measurements immediately following an infrared heating pulse has recently been developed in our laboratory.

# APPENDIX D REFERENCES


1. Nigenda, S. E.; McMillen, D. F. ; Golden, D. M., *J. Phys. Chem.*, **1988**, *93*, 1124.

2. Stewart, P. H.; Jeffries, J. B. ;Zellweger, J.-M.; McMillen, D.F.; Golden, D. M., *J. Phys. Chem.*, **1989**, *93*, 3557.

3. Shaw, R.; Walker, F. E., *J. Phys. Chem.*, **1977**, *81*, 2572.

4. See, for example,
   (a) Lloyd, S. A.; Umstead, M. E.; Lin, M. C., *J. Energ. Mat.*, **1985**, *3*, 187.
   (b) Umstead, M. E., Lloyd, S. A.; Lin, M. C., *Proc. 22nd JANNAF Combust. Mtg., CPIA*, **1985**, 512.

5. Fluornoy, J. M., *J. Chem. Phys.*, **1962**, *36*,1106.

6. (a) Korsunskii, B. L.; Dubovitskii, F. I.; Sitonian, G. V., *Dokl. Akad. Nauk SSSR*, **1967**, *174*(5), 1126.
   (b) Korsunskii, B. L.; Dubovitskii, F. I., *Dokl. Akad. Nauk SSSR*, **1964**, *1755* (2), 402.

7. Schroeder, M. A., *Proc. 16th JANNAF Comb. Mtg. CPIA*, **1978**, *82*, 644.

8. Melius, C. F.; Binkley, S. J., *Proc. 21st Symposium (International) on Combustion, 1987*; (The Combustion Institute, Pittburgh, PA, 1988) p. 1953.

9. McMillen, D. F.; Barker, J. R.; Lewis, K. E.; Trevor, P. L.; Golden, D. M., "Mechanisms of Nitramine Decomposition: Very Low-Pressure Pyrolysis of HMX and Dimethylnitramine", Final Report, SRI Project PYU-5787, June 18, 1979 (SAN 9115/117), DOE Contract EY-76-C-03-0115.

10. Wodtke, A. M.; Hintsa, E. J.; Lee, Y. T., *J. Phys. Chem.*, **1986**, *90*, 3549.

11. Tsang, W.; Robaugh, D.; Mallard, W. G., *J. Phys. Chem.*, **1986**, *90*, 5968. **1985**, *89* , 4809.

12. Gonzalez, A. C.; Larson, C. W.; McMillen, D. F.; Golden, D. M., *J. Phys. Chem.*, **1985**, *89*, 4809.

13. Saxon, R. P.; Yoshimine, M., *J. Phys. Chem.*, **1989**, *93*, 3130.

14. (a) Grieser, D. R.; Barnew, R.H., *Appl. Optics*, **1980**, *19*, 741.
   (b) Chou ,M.-S.; Dean, A. M.; Stern, D., *J. Chem. Phys.*, **1983**, *78*, 5962.

15. Barnes, R. H.; Kircher, J. F., *Appl. Optics* **1978**, *17*, 1099.

16. Alder, M.; Edner, H.; Wallin, S., Optics Lett. **1985**, *10*, 529.

17. Ozaki, T.; Matsui, Y.; Ohsawa, T., *J. Appl. Phys.*, **1981**, *52*, 2593.

18 McKenzie, R. L.; Gross, K. P., *Applied Optics*, **1981**, *20*, 2153.

19. Mele, A.; Salvetti, F.; Molinari, E.; Terranova, M. L., *J. Photochem.*, **1986**, *32*, 265.

20. (a) Mallard, W. G.; Miller, J. H.; Smyth, K. C., *J. Chem. Phys.*, **1982**, *76*, 3483.
(b) Cool, T. A.; *Appl. Optics*, **1984**, *23*, 1559.